FISEVIER

Contents lists available at ScienceDirect

# Global and Planetary Change

journal homepage: www.elsevier.com/locate/gloplacha



# Speleothem-based reconstruction of Holocene changes in monsoonal patterns and environmental conditions in Central Brazil<sup>★</sup>

Marcela Eduarda Della Libera <sup>a,b,\*</sup>, Julio Cauhy <sup>a,b</sup>, Cintia Stumpf <sup>c</sup>, Roberto V. Santos <sup>c</sup>, Francisco W. Cruz <sup>d</sup>, Nicolas M. Stríkis <sup>d</sup>, Luciana F. Prado <sup>e</sup>, Jean-Sebastian Moquet <sup>f</sup>, Michael Weber <sup>a</sup>, Rebecca Orrison <sup>g</sup>, Hai Cheng <sup>h</sup>, R. Lawrence Edwards <sup>i</sup>, Valdir F. Novello <sup>c</sup>, Hubert Vonhof <sup>b</sup>, Denis Scholz <sup>a</sup>

- <sup>a</sup> Institut für Geowissenschaften, Johannes Gutenberg-Universität Mainz, Germany
- b Max Planck Institut für Chemie, Mainz, Germany
- <sup>c</sup> Institute of Geosciences, University of Brasília, Brasília, DF, Brazil
- <sup>d</sup> Instituto de Geociências, Universidade de São Paulo, São Paulo, SP, Brazil
- <sup>e</sup> Faculdade de Oceanografia, Universidade do Estado do Rio de Janeiro, Rio de Janeiro, Brazil
- f CNRS/INSU, Institut des Sciences de la Terre d'Orléans, Orléans, France
- <sup>g</sup> Department of Atmospheric and Environmental Sciences, University at Albany, Albany, United States of America
- <sup>h</sup> Institute of Global Environmental Change, Xi'an Jiaotong University, Shaanxi, China
- <sup>1</sup> University of Minnesota, Department of Earth and Environmental Sciences, MN, United States of America

#### ARTICLE INFO

Editor: Dr. Sun Jimin

Keywords:
Paleoclimate
Paleoenvironment
Speleothems
South American Summer Monsoon
South Atlantic Convergence Zone
Tropical savanna
Precipitation Dipole
Sr isotopes
Vegetation dynamics
Holocene
South America

#### ABSTRACT

The east-west precipitation dipole that occurs in South America has been vastly investigated in previous studies using paleoclimate records from east and west of the continent, but the climate dynamics of central-eastern Brazil remains less understood. While  $\delta^{18}$ O values have been widely used to study past rainfall variability over South America, their ability to resolve local hydrological changes in central Brazil during the Holocene has been proven to be difficult. Recent studies in the region have used  $\delta^{13}$ C values and  ${}^{87}$ Sr/ ${}^{86}$ Sr ratios from speleothems to assess local paleo-hydrology and environmental conditions. Here, we revisit this topic for the last 11,000 years based on a novel multi-proxy record ( $\delta^{18}$ O,  $\delta^{13}$ C, and  ${}^{87}$ Sr/ ${}^{86}$ Sr) from a stalagmite collected in central Brazil at the northern side of the present day South Atlantic Convergence Zone (SACZ). The overall climate shifted from drier to wetter conditions throughout the Holocene, reflecting the increasing southern insolation and the monsoondriven wetting trend based on the local and regional 813C and pollen records. Changes in atmospheric circulation patterns during the Holocene might have been responsible for the increase in  $\delta^{18}$ O values through time. A north-eastern climate influence during the weaker monsoon phase from early-to-mid Holocene contrasts the late Holocene and present-day influence of SACZ over the area. Hence, a negative correlation between  $\delta^{18}$ O and  $\delta^{13}$ C indicates a decoupling of monsoon activity from local climate conditions. The Sr isotope signals in our site may be influenced by mixed lithology or increased dust input from nearby sandstone during drier periods, revealing the complexity of this proxy. The São Mateus record highlights the complex, non-stationary interplay between monsoon strength, SACZ dynamics, and atmospheric processes in shaping central Brazil's hydroclimate.

# 1. Introduction

The Brazilian savanna, or Cerrado, lies in Central Brazil and is the second-largest biome of South America. It is bordered by the Amazonian biome (rainforest) to the north and the Caatinga biome (Brazilian dry forest) to the east. The Cerrado is situated within the austral summer/

spring (October–March) precipitation regime of the South Atlantic Convergence Zone (SACZ). The SACZ is a seasonal convective band that forms in a northwest-to-southeast orientation over the continent (i.e., central Brazil – Fig. 1), and is one of the main features of the South American Summer Monsoon (SASM). It is maintained by merging two transient moisture fluxes: one following the pattern of the monsoon

 $<sup>^{\</sup>star}$  This article is part of a Special issue entitled: 'speleothem records' published in Global and Planetary Change.

<sup>\*</sup> Corresponding author at: Institut für Geowissenschaften, Johannes Gutenberg-Universität Mainz, Germany. E-mail address: marcela.godoy@mpic.de (M.E. Della Libera).

onshore flow from the north and another originating from frontal systems from the South Atlantic Ocean as they move into the continent westward (Garreaud et al., 2009; Marengo et al., 2012; Zilli et al., 2019). The overall position and intensity of the convective band changes depending on different climatic factors, such as atmospheric circulation, sea surface temperatures in the South Atlantic Ocean, low-level jets, and South Atlantic Subtropical high wind speeds (Garreaud et al., 2009; Marengo et al., 2012; Zilli et al., 2019; Wong et al., 2023).

Previous paleoclimate studies based on stalagmite oxygen isotope  $(\delta^{18}\text{O})$  records within the SASM/SACZ regime (Fig. 1a) investigated changes in the activity of both systems and their association with distinct rainfall patterns (Cheng et al., 2013; Wang et al., 2017; Campos et al., 2019; Wong et al., 2023). They define a rainfall dipole pattern between Northeastern Brazil, which primarily receives moisture from the Intertropical Convergence Zone (ITCZ) at its southernmost position, and the monsoon domain. This dipole pattern was documented at orbital (Cruz et al., 2009; Cheng et al., 2013; Deininger et al., 2019) to centennial time scales (Novello et al., 2018; Campos et al., 2019; Della Libera et al., 2022). The dipole is established when enhanced convergence in the West (Amazon) of the continent takes place (Fig. 1b), causing regional air subsidence in the Northeast, which characterizes a subsystem of the atmospheric Walker circulation known as the Bolivian High-Northeast Low system (Rodwell and Hoskins, 2001; Lenters and Cook, 1997; Sulca et al., 2016; Campos et al., 2019). However, the climate dynamics in the center of the dipole, i.e., in central-east Brazil, have not been well defined and understood yet due to the lack of archives recording the climate transition between the dipole extremes over longer time-scales, such as during the Holocene.

Over the Holocene, the dipole pattern is characterized by opposite trends of the  $\delta^{18}$ O records across tropical South America towards the Late Holocene. In western Amazonia, the tropical Andes, and southern

Brazil, increasing moisture reflected by decreasing  $\delta^{18}$ O values follows the increase in austral summer insolation (Bird et al., 2011; Bernal et al., 2016). The records from Northeastern Brazil and eastern Amazonia, on the other hand, document increasing aridity reflected by increasing  $\delta^{18}$ O values as summer insolation rises (Cruz et al., 2009; Wang et al., 2017; Utida et al., 2020). Despite the clear dipole pattern, in central-east Brazil, at the core of the dipole, climate is relatively stable from Middle-to-Late Holocene as reflected in regional  $\delta^{18}$ O records (Stríkis et al., 2011; Azevedo et al., 2021; Wong et al., 2021). It is associated with a stationary position of the central axis of the SACZ (Fig. 1a, b) over this region for the last 6000 years (Wong et al., 2021), implying a stationary influence of the SACZ in these central regions despite its apparent expansion-retraction behavior of the precipitation belt in the areas located further away from its NE-SW axis (Stríkis et al., 2011; Novello et al., 2018; Campos et al., 2019; Azevedo et al., 2021).

A monitoring program performed for two years in São Bernardo cave (~10 km from São Mateus cave) by Moquet et al. (2016) shows a significant negative correlation between local rainfall amount and  $\delta^{18} O_{precip}$  at both monthly and weekly scales showing that on short time scales,  $\delta^{18} O$  does predict rainfall amounts. However, paleo-records from central Brazil suggest that the long-term variability of  $\delta^{18} O$  records do not record rainfall amounts so easily (Wortham et al., 2017; Novello et al., 2019; Ward et al., 2019; Azevedo et al., 2021). This likely relates to the existence of multiple large-scale atmospheric processes related to the monsoon, including mixing between different moisture sources and Rayleigh distillation processes. Such processes likely vary significantly on longer time scales, affecting  $\delta^{18} O$  values of rainfall, and thus confound any rainfall amount effects recorded in modern rainfall  $\delta^{18} O$  values (Ampuero et al., 2020).

Therefore, recent multi-proxy studies investigate paleo-hydroclimate and paleoenvironmental changes in central Brazil using speleothem  $\delta^{13} \mathrm{C}$ 

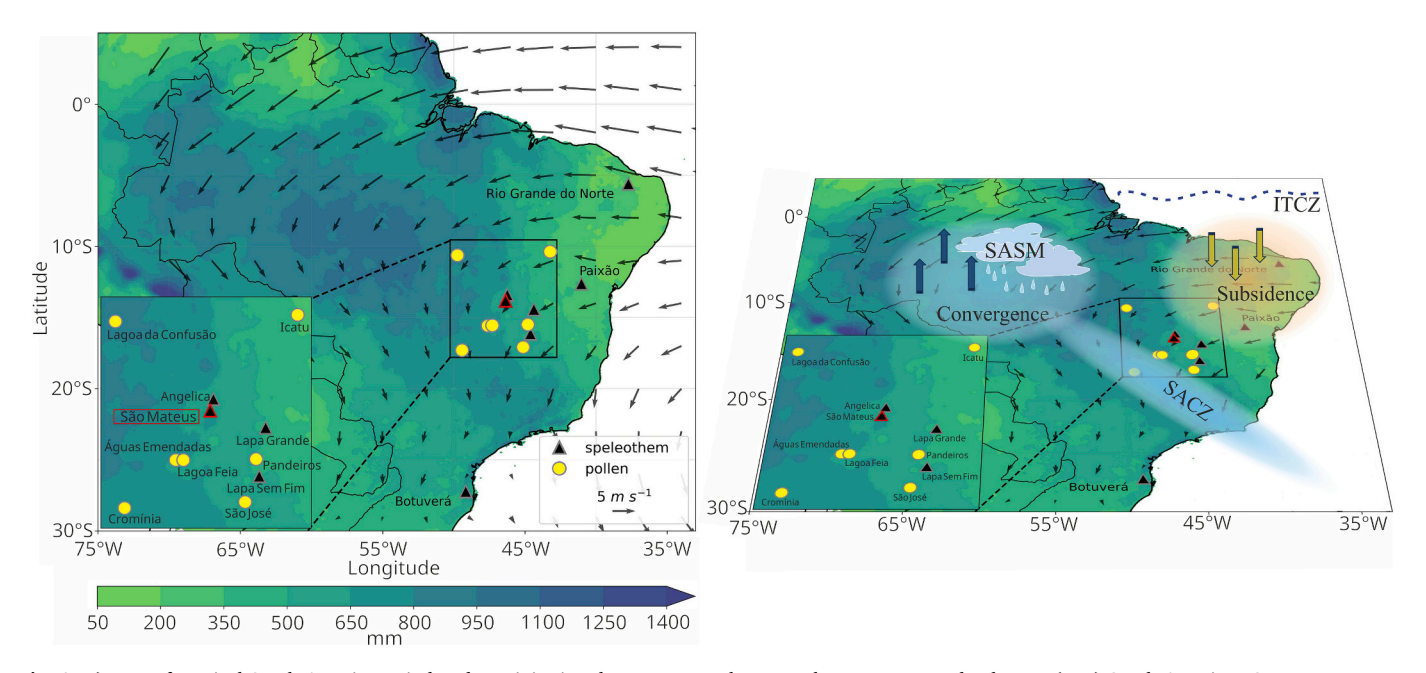


Fig. 1. a) Map of tropical South America. Wind and precipitation data represent the December, January, and February (DJF) South American Summer Monsoon features for the forty-year climatology covering the period between 1981 and 2020 CE. The years correspond to the December month of the DJF season, i.e., D(0), J (+1), F(+1). Low-level (850 hPa) horizontal wind data (u, v) were derived from the ERA5 reanalysis. Total seasonal precipitation data were derived from the CHIRPS-2.0 dataset, a gridded rainfall time series based on rain gauges (Hersbach et al., 2020; Funk et al., 2014). The triangle with the red borders represents the location of São Mateus cave. The other triangles represent the following cave sites: Rio Grande do Norte (Cruz et al., 2009); Paixão cave (Stríkis et al., 2015); Angelica cave (Wong et al., 2021); Lapa Sem Fim cave (Azevedo et al., 2021); Lapa Grande cave (Stríkis et al., 2011); Botuverá cave (Wang et al., 2007). The yellow circles are pollen and lake sediment records mentioned in the text: Águas Emendadas (Barberi et al., 2000); Lagoa Feia (Cassino et al., 2020); Cromínia (Salgado-Labouriau et al., 1997); São José (Cassino et al., 2018); Lagoa da Confusão (Behling, 2002); Icatu (De Oliveira et al., 1999); Pandeiros wetland (Sabino et al., 2021). b) Same as a), but with a representation of the precipitation dipole between central and northeast South America. The climatological DJF location of the ITCZ is represented by the black dashed line. (For interpretation of the references to colour in this figure legend, the reader is referred to the web version of this article.)

and 87Sr/86Sr records to elucidate local hydrological conditions (Wortham et al., 2017; Campos et al., 2019; Ward et al., 2019; Azevedo et al., 2021). Overall, these studies suggest that local precipitation in the central parts of Brazil was indeed decoupled from continental monsoon patterns over long-time scales, either due to changes in moisture sources or Rayleigh distillation processes. For instance, Ward et al. (2019) indicate that changes in monsoon intensity at its core may not directly reflect local precipitation amounts downstream (i.e., in central Brazil) based on their  $^{87}\text{Sr}/^{86}\text{Sr}$  and  $\delta^{13}\text{C}$  records used as proxies for local hydrology. Additionally, Wortham et al. (2017) suggest that moisture contributions from the South Atlantic Ocean at sites closer to the coast than the core monsoon region dilute the monsoon signal derived from upstream dynamics. This is reflected by rising 87Sr/86Sr values, suggesting an increase in moisture, during overall stable monsoon  $\delta^{18}O$ records in central Brazil (Wortham et al., 2017). This decoupling has also been brought up in a recent review study by Gorenstein et al. (2022), which compiled 173 studies from South America based on different paleo-archives (speleothems, sediment cores and soil samples), from which a wide selection of proxies was analyzed (e.g.,  $\delta^{18}$ O,  $\delta^{13}$ C, pollen, mineralogy, grain size, trace-elements). They point out that the paleoclimate records from central-eastern Brazil show the least consistent picture amongst each other and indicate a high variability of the SACZ central axis position during Middle Holocene. This again suggests a decoupling of local moisture conditions in central-eastern Brazil from the overall intensity of the SASM.

Here we present a new speleothem multi-proxy record from central-eastern Brazil based on  $\delta^{18} O$  and  $\delta^{13} C$  values as well as  $^{87} \text{Sr}/8^{66} \text{Sr}$  ratios from São Mateus cave (Fig. 1a), covering the entire Holocene. This is the longest continuous Holocene record from the region so far. We reconstruct the spatiotemporal evolution of the dipole climate transition happening at our study site and discuss the changes in the local environment.

# 2. Site and sample description

São Mateus cave (13.67° S; 46.37° W, 623 m a.s.l. - Fig. 1a) is located at the State Park of Terra Ronca (PETER), Goiás state, Central Brazil. The cave is developed in Neoproterozoic karstified dolostone interbedded with limestones of the Sete Lagoas Formation, Bambuí Group (Dardenne, 1978; Auler and Farrant, 1996). In this area, large underground cave systems were formed by drainages flowing westwards from the topographically higher sandstones of the Urucuia Group (Campos and Dardenne, 1997), which forms the Serra Geral Plateau ca. 15 km to the east of the cave site (Supp. Fig. 1). The caves were formed by the weathering of the carbonate unit along the trajectory of these rivers (Dardenne, 1978; Auler and Farrant, 1996), such as the São Mateus River. The São Mateus cave system intersects three sedimentary packages: one characterized by doloarenites and recrystallized dolomitic limestone, a second one by intercalations of laminated argillaceous limestones and siliciclastic rocks ranging from claystone to siltstones, and a third package dominated by laminated quartzose siliciclastic rocks, with interbeds of massive to laminated siltstones and very fine to fine sandstones, along with subordinate marly limestones (Supp. Fig. 2) (Governo do Estado de Goiás, Secretaria de Meio Ambiente e Desenvolvimento Sustentável, and STCP Engenharia de Projetos Ltda, 2016).

The present-day climate in PETER is characterized as tropical semihumid, presenting a seasonal pattern of precipitation with wet summer and dry winter seasons. Based on the records of the meteorological station São Vicente ( $\sim$ 14 km from São Mateus cave), the mean annual precipitation between 1974 and 2023 is 1428 mm yr $^{-1}$ . Most of the rainfall (80 %) occurs between October and April during the summer monsoon season and the SACZ active period, feeding the karst aquifer above São Mateus Cave.

The local vegetation is generally characterized as Cerrado (Brazilian savanna), which contains many sub-categories. Karstic areas within the Cerrado biome can present a type of vegetation assembly known as

"Mata Seca Decidua" (dry deciduous forest) or "Mata Calcaria" (calcareous forest). Such vegetation can develop on a thin soil cover (~30 cm), changes dramatically between dry and wet seasons, and is highly affected by water availability. The arboreal coverage is 60–90 % during the wet season, and 15–35 % in the dry season. The surface also exhibits calcareous rock pavements with epikarst features, such as dissolution pools, which may accumulate organic matter and soil.

The current study is based on stalagmite SMT16 collected in São Mateus cave at the 700 Hall (Salão Setecentos), which is located ca. 150 m away from the cave entrance (Supp. Fig. 2), and ca. 30 m above the modern level of the São Mateus River. The 404 mm-long speleothem section used in this study is a cylindrical aragonite stalagmite formed by acicular crystals without signs of recrystallization (Fig. 2b).

#### 3. Methods

# 3.1. Chronology and stable isotopes

A total of 18 <sup>230</sup>Th/U-ages were determined along the growth axis of SMT. For each sample, ~100 mg of carbonate powder was hand-drilled and collected for the separation of the U and Th fractions (Edwards et al., 1987). These fractions were then further analyzed using multi-collector inductively coupled plasma-mass spectrometry (MC-ICP-MS) at the Geochronology Laboratory at the University of Minnesota (USA) and at the Institute of Global Environmental Change, Xi'an Jiaotong University (China), following the methods described in Cheng et al. (2013a). The final chronology was established by calculating an age-depth model using StalAge (Scholz and Hoffmann, 2011).

For  $\delta^{18}O$  and  $\delta^{13}C$  analysis, a total of 1320 samples of powdered carbonate were collected along the stalagmite growth axis with a constant spacing of 0.3 mm between samples using a Sherline Mill device with a 0.1 mm drill bit. The analyses were performed at the Laboratory of Stable Isotopes at the Institute of Geoscience of the University of São Paulo (LES-USP) and at the Laboratory of Geodynamic, Geochronological and Environmental Studies of the University of Brasilia (LEGGA -UnB). At LES, a Thermo-Finnigan Delta Plus Advantage mass spectrometer coupled to a Gas Bench online sample preparation system was used, and at LEGGA, a Thermo MAT 253 attached to a Kiel IV Carbonate. Both oxygen and carbon isotope ratios are expressed in  $\delta$ -notation, on the Vienna Pee Dee Belemnite (VPDB) scale with the per mil deviation from VPDB calculated using the following equation:  $\delta^{18}O$  = [(( $^{18}\text{O}/^{16}\text{O})_{\text{sample}}$  / ( $^{18}\text{O}/^{16}\text{O})_{\text{VPDB}}$ ) - 1] × 10<sup>3</sup> (example equation for the oxygen isotope values). Analytical uncertainties (1SD) based on the reproducibility of routinely measured in-house standards is 0.1 % for both analyses.

# 3.2. Strontium isotope analysis

The <sup>87</sup>Sr/<sup>86</sup>Sr isotope ratios were determined for the speleothem as well as carbonate host rock and soil samples, the latter two being potential end members for the Sr isotope ratios in the stalagmite. <sup>87</sup>Sr/<sup>86</sup>Sr ratios of SMT16 were analyzed by both solution and laser ablation (LA) mass spectrometry (Supp. Table 1) at LEGGA-UnB and Johannes-Gutenberg University (JGU) Mainz, respectively. Globally recognized reference materials were used for calibration of the analysis. NIST SRM987 was used to normalize solution-based MC-ICP-MS data (Supp. Table 2). Laser ablation MC-ICP-MS data were calibrated against NanoSr as the main reference material, with JCt-1 and JCp-1 acting as quality controls (Supp. Table 1). The 87Sr/86Sr ratios obtained from all three reference materials fell within the range of published solution-based values (Weber et al., 2018, 2020). The results from the two techniques (solution MC-ICP-MS and LA-MC-ICP-MS) are directly comparable due to the uniformity of the calibration procedures. Given the compatibility between these methods, the results of the LA-MC-ICP-MS method will be taken as the main record due to the higher resolution. Further details can be found in Supplementary Text 1.

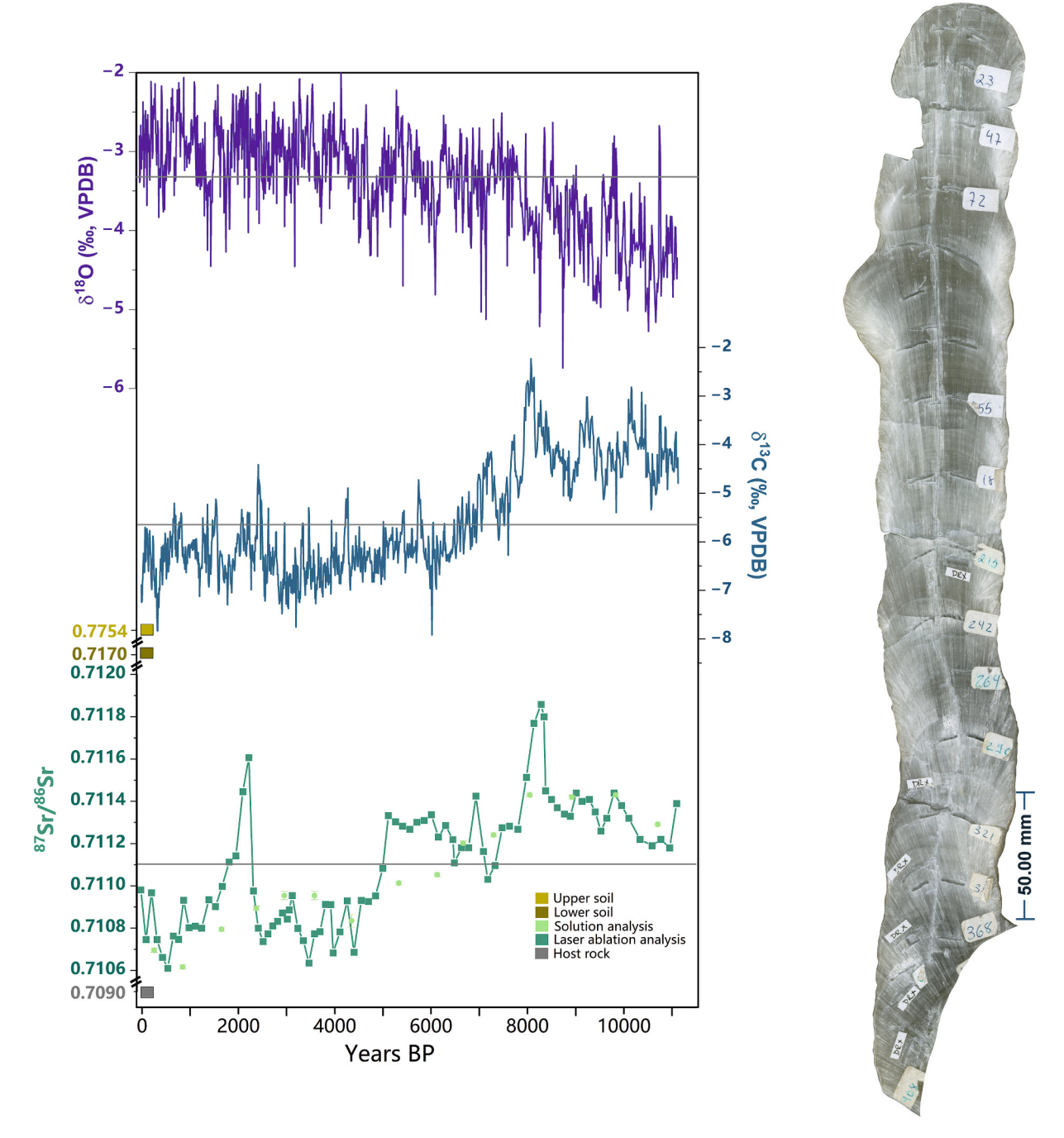


**Fig. 2.** a) SMT16  $\delta^{18}$ O (purple),  $\delta^{13}$ C (blue), and  ${}^{87}$ Sr/ ${}^{86}$ Sr records. Dark green squares represent laser ablation analyses; light green circles represent solution analyses. The yellow, brown, and gray squares show the  ${}^{87}$ Sr/ ${}^{86}$ Sr isotope ratios of the upper and bottom soil samples and the host rock, respectively. The light gray line is the mean value of each proxy record. b) Stalagmite SMT16. (For interpretation of the references to colour in this figure legend, the reader is referred to the web version of this article.)

# 3.3. Back-trajectory and clustering analysis

Back-trajectories initiating at the location of São Mateus cave (13.67° S; 46.37° W, 623 m a.s.l.) were computed between 2012 and 2019 using the Hybrid Single-Parcel Lagrangian Integrated Trajectory model 5 (Hysplit V5.3.0; Stein et al., 2015; Rolph et al., 2017). Back trajectories were calculated daily at a local time of 13 h. Since the most important moisture transport occurs in the lower troposphere, the starting height for the trajectories was set at 1500 m a.s.l. (~850 hPa) and 7 days were considered to track back air parcels. According to Ampuero et al. (2020), the 7-day back trajectories can trace the pathway

of an air mass back to the point where it was last saturated. This timeline allows us to consider the relevant isotopic fractionation processes that occur during atmospheric moisture transport (Hurley et al., 2012; Ampuero et al., 2020). ERA 5 data were used to run the model (Hersbach et al., 2020) with a spatial resolution of  $0.75^{\circ} \times 0.75^{\circ}$  and a time step of 6 h starting at 0:00 UTC. The back-trajectories were chosen if they started on precipitating days and if their numerical error was within tolerance (Ampuero et al., 2020). Days with precipitation were defined as days with local precipitation higher than 1 mm computed with data from the Global Precipitation Measurement (GPM; Huffman et al., 2023) at a spatial resolution of  $0.25^{\circ} \times 0.25^{\circ}$ , with 25 tiles. A total of 681 back-

trajectories were selected.

#### 4. Results

# 4.1. <sup>230</sup>Th/U-dating

All  $^{230} Th/U$ -ages determined for stalagmite SMT (Supp. Table 3) have an average  $2\sigma$ -uncertainty of 0.23 %, yielding a very well-constrained chronology (Supp. Fig. 3). Generally high  $^{230} Th/^{232} Th$  isotope ratios throughout the sample document that detrital contamination does not have a significant influence on the final ages, except for two samples, SMT16–2 and SMT16–378. Additional details are presented in Supplementary Table 3. Based on the age model, SMT16 spans the entire Holocene between 11,078- and 24-years BP (Supp. Fig. 3). In general, SMT16 shows a relatively stable growth rate with an average value of 32  $\mu m/yr$  until the Middle Holocene, followed by an increase to 43  $\mu m/yr$  during the Late Holocene (i.e., after 4000 years BP, Supp. Fig. 3).

# 4.2. $\delta^{18}O$ and $\delta^{13}C$ values

The stable isotope records ( $\delta^{18}O$  and  $\delta^{13}C$  – Fig. 2a) have an average temporal resolution of 8 years. The  $\delta^{18}O$  record shows a steady trend to higher values towards the present with values from -5.4 to -2.1 ‰. The lowest values are observed in the oldest part of the record during the Early Holocene (11700–8200 years BP) with a mean value of -4 ‰ (Fig. 2a). After a negative excursion centered at 8225 years BP, the values increase marking the transition from the Early to the Middle Holocene. The Middle Holocene (8200–4200 years BP) values range around the record mean of -3.3 ‰ until 4305 years BP. At the transition to the Late Holocene (4200 years BP to the present), the values further increase until the present, with a mean value of -2.9 ‰.

In contrast to the oxygen isotopes, the  $\delta^{13}$ C record is marked by a trend to more negative values towards the present with a range between -7.9 to -2.2 ‰. The highest  $\delta^{13}$ C values of the record are observed from 11,078 to 7882 years BP. Subsequently, the  $\delta^{13}$ C record shows a gradual decrease until  $\sim$ 2800 BP followed by a stationary trend until the present. There is an overall negative correlation between the  $\delta^{13}$ C and  $\delta^{18}$ O time series (r=-0.5, p<0.01) for the entire period (Supp. Fig. 4). However, a spearman's running correlation with a window size of 150 data points representing a temporal resolution of  $\sim$ 1233 years shows that these two proxies show a positive correlation (yet varying) from  $\sim$ 6800 BP until the present, evidencing a coupling for most of the Holocene (Supp. Fig. 5). Yet, the negative correlation from  $\sim$ 9500–7250 BP indicates a decoupling at the beginning of the period. The cave host rock has a mean value of -2.9 ‰.

# 4.3. <sup>87</sup>Sr/<sup>86</sup>Sr values

The <sup>87</sup>Sr/<sup>86</sup>Sr record of SMT (Fig. 2a) is composed of 87 data points ranging from 0.71061 to 0.71186. The highest values are observed within the oldest portion of the stalagmite between 11,000- and 7900-years BP, peaking at 8200 years BP. Subsequently, until ca. 5000 years BP, the ratios show a plateau with lower values. This is followed by a distinct decrease to generally lower values until the present, with a prominent positive excursion centered at 2213 years BP.

The cave host rock has a mean value of 0.70905, which is much less radiogenic (i.e., lower  $^{87}\text{Sr}/^{86}\text{Sr}$  values) than both soil samples. The upper soil sample ( $^{87}\text{Sr}/^{86}\text{Sr}=0.77545\pm0.00001)$  is more radiogenic than the bottom one ( $^{87}\text{Sr}/^{86}\text{Sr}=0.71703\pm0.00001)$ . Thus, the Sr isotope ratio of the stalagmite lies between the soil and host rock values (Fig. 2).

To determine the correlation between  $^{87}\text{Sr/}^{86}\text{Sr}$  and the higher-resolution  $\delta^{18}\text{O}$  and  $\delta^{13}\text{C}$  records, they were down-sampled to the same number of data points as the lower-resolution strontium isotope record (87 points). The values obtained from the  $\delta^{18}\text{O}$  and  $\delta^{13}\text{C}$  records

were matched on the depth-scale with the corresponding data points of the  $^{87}\text{Sr}/^{86}\text{Sr}$  record. We observe a positive correlation of 0.71 (p < 0.001) with the  $^{813}\text{C}$  record and a negative correlation of -0.45 (p < 0.001) with the  $^{18}\text{O}$  values (Supp. Fig. 4).

# 4.4. Back trajectories and clustering analysis

The back-trajectory analysis for the period between 2012 and 2019 at São Mateus cave mainly shows atmospheric transport pathways from the east (73 %) and the north-east (23 %). Both trajectories are associated with the months of higher rainfall contribution at São Mateus between October and March and contribute approximately equally throughout the year, but the eastern cluster has a much higher contribution to the total amount of trajectories during JFM (Supp. Fig. 6). Between May and September, there are little to no trajectories, especially from the eastern cluster.

#### 5. Discussion

# 5.1. General understanding of proxy signal controls

# 5.1.1. Carbon isotopes

Changes in speleothem  $\delta^{13}$ C values are influenced by several factors, such as vegetation type (C<sub>3</sub> vs. C<sub>4</sub>) and density above the cave, soil biogenic activity (CO<sub>2</sub> production) versus host-rock δ<sup>13</sup>C contribution, if the dissolution of the carbonate host-rock is an open, closed or intermediate system, and prior carbonate precipitation (PCP), all related to local climate conditions (McDermott, 2004; Fohlmeister et al., 2011; Novello et al., 2021). In general, drier conditions result in higher  $\delta^{13}$ C values due to sparser, savanna-type  $C_4$  vegetation (-9 % to -17 %) and reduced soil CO2 (Gouveia et al., 2002; Pessenda et al., 2010), longer water residence times (increased PCP, Fairchild and Baker, 2012; Fohlmeister et al., 2020), and increased host-rock contribution (Novello et al., 2021 and references therein). Conversely, wetter conditions result in lower  $\delta^{13}$ C values via denser, forest-type C<sub>3</sub> vegetation (-32 % to −20 ‰), increased soil CO<sub>2</sub>, reduced PCP, and lower host-rock input. In an open system, the percolating water is constantly interacting with the soil air, an infinite reservoir  $CO_2$ , which leads the  $\delta^{13}C$  to reflect the isotopic composition of the soil CO2. In a close system, the percolating water is separated from the soil CO<sub>2</sub> and the initial amount of CO<sub>2</sub> in the solution is progressively consumed by the dissolution of the carbonate host-rock, which is reflected in the final  $\delta^{13}$ C isotopic composition. In natural environments, it is uncommon that systems operate fully open or close, but rather that the interaction between the percolating water and the host-rock happens in an intermediate state between the two extremes (McDermott, 2004; Fohlmeister et al., 2011; Novello et al.,

A study by Novello et al. (2021) using a compilation of 25 stalagmites from tropical South America that cover the last 2000 years shows that the sites within this broad region share similar characteristics in their  $\delta^{13}C$  records: an average  $\delta^{13}C$  value below -6% and most of them show a positive correlation between their  $\delta^{13}C$  and  $\delta^{18}O$  values (r ranging from 0.20 to 0.56). This correlation indicates that local hydrology was closely associated with the monsoon at most of the sites (documented by the  $\delta^{18}O$  values). The dominant  $d^{13}C$  value of -6% was attributed to the prevailing  $C_3$  vegetation above most karst systems. This is in agreement with the  $d^{13}C$  values below -6% during the Middle-to-Late Holocene in SMT16 (6000 BP until the present) and the observed r values between the SMT16  $\delta^{13}C$  and  $\delta^{18}O$  ranging from 0.2 to 0.5 for the same period (Supp. Fig. 5).

# 5.1.2. Strontium isotopes

Strontium isotope ratios (<sup>87</sup>Sr/<sup>86</sup>Sr) reflect changes in the relative contribution of different Sr sources with distinct <sup>87</sup>Sr/<sup>86</sup>Sr values fed by the percolating water into the speleothem (Banner et al., 1996; Weber et al., 2018). Therefore, they are commonly used as a proxy for local

hydrology due to the relative contribution of the two main Sr sources of the drip water: Sr leached from the carbonate host rock and from the soils overlying the host rock (Banner et al., 1996; Weber et al., 2018). The soil usually shows more radiogenic (higher) <sup>87</sup>Sr/<sup>86</sup>Sr ratios compared to the less radiogenic (lower) values of the carbonate host rock, resulting in an intermediate value between the two end-members in the speleothem. It is often suggested that during wetter conditions, the infiltrating water drains faster through the carbonate host rock, resulting in less leaching, and thus a more radiogenic signal in the speleothem, closer to the <sup>87</sup>Sr/<sup>86</sup>Sr ratio acquired from the overlying soil. Conversely, drier conditions lead to a longer residence time of the percolating water in the carbonate host rock, leading to more leaching and thus less radiogenic values in the speleothems (Banner et al., 1996). So far, various studies in Brazil have interpreted the variation in speleothem <sup>87</sup>Sr/<sup>86</sup>Sr values in that framework (Novello et al., 2019; Utida et al., 2020; Azevedo et al., 2021). Yet, as it will be discussed in section 5.2, the SMT16 Sr isotope record shows a non-conventional pattern that differs from this common hydrological interpretation, likely reflecting different processes that influence the final Sr values in SMT16. Other mechanisms that have been suggested for variation in speleothem <sup>87</sup>Sr/<sup>86</sup>Sr values are shifts in the percolating water flow routes (different porosity and permeability, Banner et al., 1996; Wortham et al., 2017) and inputs of eolian dust to the overlying soils (Banner et al., 1996; Goede et al., 1998; Frumkin and Stein, 2004; Torfstein et al., 2018). The latter studies, despite being from different geological contexts including desert and non-desert regions, associate drier conditions to higher dust mobilization and deposition yielding more radiogenic <sup>87</sup>Sr/<sup>86</sup>Sr values. In such a scenario, greater aridity, reduced vegetation cover, and changes in wind lead to increased eolian dust transport, while during wetter conditions, increased vegetation cover and moisture limits dust mobilization, yielding lower 87Sr/86Sr values, closer to the host rock (Banner et al., 1996; Frumkin and Stein, 2004; Torfstein et al., 2018).

# 5.1.3. Oxygen isotopes

Speleothem δ<sup>18</sup>O records in tropical South America are associated with the isotopic signature of the rainfall, which is strongly related to the monsoon system. Within the SACZ region, the amount of local precipitation (i.e., the amount effect) is an important process affecting rainfall  $\delta^{18}$ O values. More (less) local precipitation leads to lower (higher)  $\delta^{18}$ O values, thus resulting in an anti-correlation with local rainfall amount (Vuille et al., 2012; Moquet et al., 2016; Della Libera et al., 2022). This is a common process in areas within the SASM, such as in central Brazil. This is demonstrated by the monitoring program performed in the nearby cave of Sao Bernardo (Moquet et al., 2016). The authors show that speleothem  $\delta^{18}$ O values are anti-correlated with the average DJFM precipitation amount (r = -0.66) as well as the average annual precipitation amount (r = -0.45) for the past century. This monitoring also showed that the mean dripping water value ( $-4.2 \pm 0.1$  % VSMOW, n= 37) during the monitoring period (1.5 years) did not change significantly, thus evidencing that there is in fact a minimum 1.5-year residence time of the water in the aquifer. Therefore, the drip water  $\delta^{18}O$ represents the weighted annual mean of the rainfall  $\delta^{18}$ O and, since most of the recharge occurs during the wet season, the drip water primarily reflects the rainfall  $\delta^{18}\mbox{O}$  signature of the wet summer months.

Additionally, the current understanding of rainfall  $\delta^{18}$ O values in the SASM regime is that these are dominated by Rayleigh distillation and influenced by convective processes associated with monsoon activity (Ampuero et al., 2020; Orrison et al., 2022). Heavier oxygen isotopes ( $^{18}$ O) are preferentially removed from the air mass along its trajectory through precipitation, resulting in a progressive depletion of the remaining air mass (i.e., in more negative  $\delta^{18}$ O values, Ampuero et al., 2020; Orrison et al., 2022). Therefore, rainfall  $\delta^{18}$ O values in the SASM domain are also affected by the degree of rainout upstream that along the air mass trajectory from the tropical Atlantic into the continent (Fig. 1). As the air mass moves further inland, it becomes progressively more depleted in  $^{18}$ O (Vuille et al., 2012; Ampuero et al., 2020). This

leads to an isotope effect in rainfall that is unrelated to the amount of rainfall on the study site (Ampuero et al., 2020; Della Libera et al., 2022; Orrison et al., 2022). Therefore, a direct assessment of local hydrology exclusively using oxygen isotopes may be difficult due to multiple other processes potentially influencing the  $\delta^{18}$ O values.

# 5.1.4. Potential effects of changes in seasonality

Strong seasonality is a major characteristic of the hydroclimate in the Cerrado and thus has a major impact on its vegetation. Thus, it is important to discuss the possible implications for our proxy records. Both the total amount of wet season rainfall and the distribution of precipitation (season length, number of rainy days, intensity and length of dry spells) will have an impact on vegetation, soil moisture and infiltration (Bustamante et al., 2012; Klink et al., 2020; Hofmann et al., 2023). However, rainfall distribution has a stronger impact on tree grass changes in the Cerrado, given that a pronounced dry season determines fuel accumulation and fire frequency, and that the resulting fire regime strongly shapes the tree-grass balance (Bustamante et al., 2012; Klink et al., 2020; Hofmann et al., 2023). Therefore, even if the total amount of the wet season rainfall remains similar, the crucial factor might be the relative duration between wet and dry season. For instance, more clustered rainfall events in the wet season imply longer dry spells, which would result in a higher fire risk and favor grasses over trees (Bustamante et al., 2012; Klink et al., 2020; Hofmann et al., 2023).

As  ${\sim}80$  % of precipitation occurs during the wet season (monsoon), our SMT16  $\delta^{18}{\rm O}$  record is strongly biased towards the wet season and thus represents changes in both wet season precipitation amounts and large-scale SASM/SACZ variability (see section 5.1.3). Yet, the  $\delta^{18}{\rm O}$  signal is smoothed in the aquifer and reflects the weighted mean of the rainfall signal of several years (Moquet et al., 2016). In contrast,  $\delta^{13}{\rm C}$  values and Sr isotopes will respond more directly to the local hydrology because both proxies are influenced by environmental factors, such as vegetation dynamics, soil moisture, and prior calcite precipitation, which are all more affected by the length of the dry season.

In summary, even if the observed trends between the different proxies are not similar, this divergence may provide important information on the seasonal distribution of rainfall. For instance, intervals showing more positive  $\delta^{13} \text{C}$  values and evidence of C4 vegetation expansion could be interpreted as phases of prolonged dry seasons, even when the  $\delta^{18} \text{O}$  values indicate a relatively stable or strong wet season precipitation. Thus, the proxies dominated by local hydrology ( $\delta^{13} \text{C}$  and Sr isotopes) are more responsive to the length of the dry season, which directly affects vegetation cover and fire regimes in the Cerrado.

# 5.2. Environmental changes in Central-Eastern Brazil during the Holocene

The general trend of the SMT16  $\delta^{13} C$  record, i.e., higher values at the beginning of the Holocene from 11,000 to 7500 BP followed by a distinct decrease and stabilization at lower values towards the present, is also observed in nearby stalagmite records from Lapa Sem Fim (LSF – Azevedo et al., 2021) and Lapa Grande (LG – Stríkis et al., 2011) (Fig. 3c). The strong agreement between the SMT16  $\delta^{13} C$  record and these records indicates a widespread regional change in the environmental conditions and vegetation throughout the Holocene. This trend in  $d^{13} C$  values may reflect a progressively wetter climate (i.e., more precipitation in the wet season and/or longer wet seasons) and an increase in vegetation density in the Late Holocene (lower  $\delta^{13} C$  values) compared to a drier Early Holocene (higher  $\delta^{13} C$  values).

The stratigraphically well-constrained pollen record of Lagoa Feia core ( $\sim$ 250 km SW of São Mateus cave, Fig. 1 and 4d, Cassino et al., 2020; Escobar-Torrez et al., 2024) also points to generally drier climate during the Early Holocene until  $\sim$ 7200 BP in the region, indicating that this period was marked by a series of dry episodes interspersed with wetter ones (Cassino et al., 2020). The authors also performed a PCA analysis to access regional patterns of vegetation variability in Central Cerrados based on the pollen records of Lagoa Feia (Cassino et al., 2020),

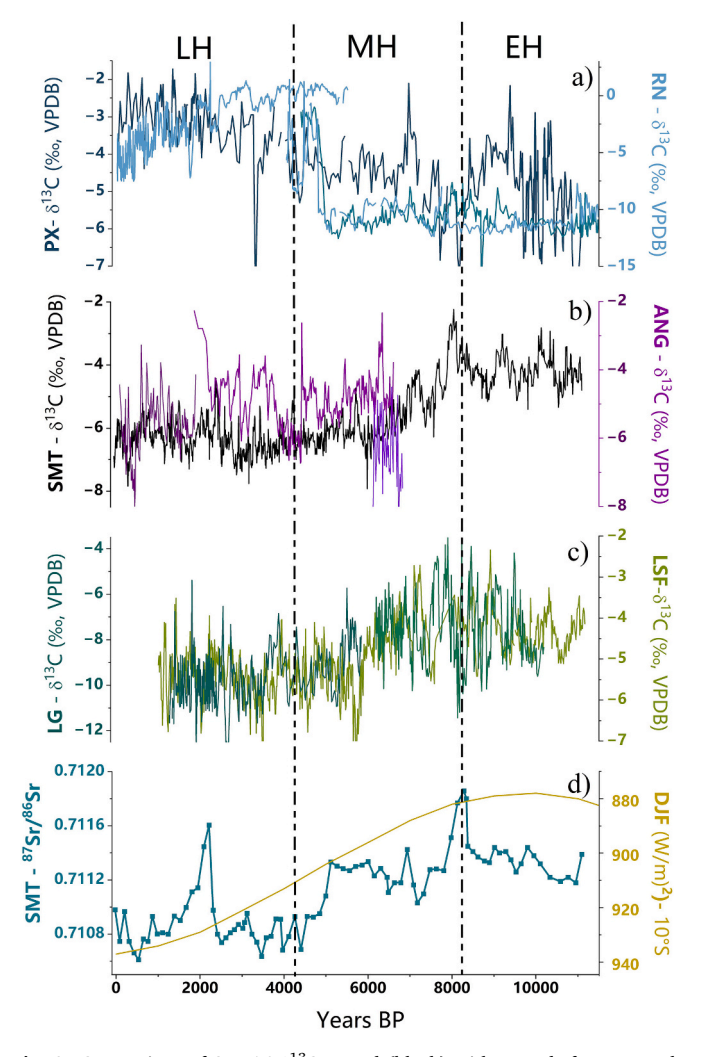


**Fig. 3.** Comparison of SMT16  $\delta^{13}$ C record (black) with records from central-eastern and Northeastern Brazil. a) Rio Grande do Norte cave (Cruz et al., 2009) and Paixão cave (Stríkis et al., 2015) in northeastern Brazil region; b) Angelica cave (Wong et al., 2021) and São Mateus cave (this study) in central-eastern Brazil; c) Lapa Grande cave (Stríkis et al., 2011) and Lapa Sem Fim cave (Azevedo et al., 2021) in central-eastern Brazil; d) SMT16  $^{87}$ Sr/ $^{86}$ Sr record with the DJF insolation for  $10^{\circ}$ S (Berger and Loutre, 1991). The dashed lines separate between the Early, Middle and Late Holocene periods, here as EH, MH, LH, respectively.

São José (Cassino et al., 2018) and Salitre (Ledru et al., 1996) (Fig. 4c) that also evidences this drier period with wet events during the Early Holocene (Cassino et al., 2020). Similar variations are visible in the SMT16 δ<sup>13</sup>C record during the Early Holocene suggesting rapid environmental shifts (Fig. 4b). Other pollen studies from central Brazil confirm that conditions during the Early Holocene were generally dry, such as Águas Emendadas (Barberi et al., 2000), Cromínia (Salgado-Labouriau et al., 1997), São José (Cassino et al., 2018), and Lagoa da Confusão (Behling, 2002) (Fig. 1), but most of these records have a low temporal constrain. Therefore, we take Lagoa Feia pollen data, along with the general understanding of the other pollen records, to support the hydroclimatic interpretation of the SMT16, LG, and LSF speleothem records, suggesting a reduction in the length and intensity of the rainfall seasons and generally more severe dry seasons during the Early Holocene during a period of weakened SASM (Bernal et al., 2016: Cassino et al., 2020).

The major transition observed in the SMT16  $\delta^{13}$ C record to more negative values occur in the Middle Holocene after its largest excursion at ~8000 BP. The shifts in the LG (~7900 BP) and LSF (~7200 BP)  $\delta^{13}$ C

records show a broadly similar timing (Fig. 3), which might indicate a regional increase in vegetation density and  $C_3$  plants. The Lagoa Feia pollen data corroborate this transition to increased humidity with the onset of aquatic plants, higher and more stable lake levels, and a higher occurrence of forest-type taxa (Cassino et al., 2020). This change in vegetation during the Middle Holocene was likely triggered by the initial increase in humidity in the SASM regions due to increasing austral summer insolation ( $10^{\circ}$ S), therefore providing more uniform rainfall seasons and shorter dry ones (Cruz et al., 2009; Bernal et al., 2016; Smith and Mayle, 2018).

The further increase in summer insolation might have favored similar-to-wetter conditions during the Late Holocene. The lower  $\delta^{13}C$ values ( $\sim -5$  % or lower) in SMT16, LSF, LG, and Angelica cave (ANG – Wong et al., 2021, Figs. 1 and 3) suggest an overall more stable precipitation regime and environment with denser vegetation, higher abundance of C<sub>3</sub>-plants (Novello et al., 2021), and less variable climate conditions compared to the Middle and Early Holocene (Fig. 3). The pollen record of Lagoa Feia (Fig. 4d) shows a broad expansion of the woody Cerrado vegetation and a sharp rise in water level-associated taxa (Escobar-Torrez et al., 2024). In addition, the Pandeiros wetland (Sabino et al., 2021) also suggests a generally wetter Late Holocene, even though short-term dry events are present throughout the period. This overall coherence amongst different records highlights the transition to relatively wetter climate throughout the year (i.e., shorter dry seasons) and a landscape with more dense vegetation after the Middle Holocene in central-eastern Brazil.

Based on this interpretation of the speleothem  $\delta^{13}C$  record, we can now assess the Sr isotope data in some more detail. The striking positive correlation (r=0.7, p<0.01 – Fig. 2, Supp. Fig. 4) between the SMT16  $\delta^{13}C$  and Sr isotope records suggests that wetter conditions generally resulted in lower speleothem  ${}^{87}Sr/{}^{86}Sr$  ratios. This is clearly at odds with the classical interpretation of  ${}^{87}Sr/{}^{86}Sr$  ratios in speleothems (Banner et al., 1996, compare section 5) applied in previous studies from South America using both proxies (Novello et al., 2019; Utida et al., 2020) or the ones using  ${}^{87}Sr/{}^{86}Sr \cdot \delta^{18}O$  comparisons (Wortham et al., 2017; Ward et al., 2019 – see Supp. Tex. 2). In that classical interpretation, drier conditions lead to more carbonate host-rock Sr contribution to cave drip water, and therefore to lower speleothem  ${}^{87}Sr/{}^{86}Sr$  ratios. This explanation does not work for the SMT16 record, which shows a positive correlation between  $\delta^{13}C$  and  ${}^{87}Sr/{}^{86}Sr$ , hence higher  ${}^{87}Sr/{}^{86}Sr$  ratios at increased aridity.

In our study, the long-term in-phase relationship between <sup>87</sup>Sr/<sup>86</sup>Sr and  $\delta^{13}$ C values suggests that the above mechanisms are unable to explain the SMT16 signals, at least on this time-scale. Since the  $\delta^{13}$ C record agrees well with records at other localities (LG, LSF) and has a relatively straightforward hydroclimatic interpretation, it appears that the  ${}^{87}\mathrm{Sr}/{}^{86}\mathrm{Sr}$  signal at SMT16 differently responds to hydroclimate change than at other sites. One explanation for higher <sup>87</sup>Sr/<sup>86</sup>Sr during drier periods is that variations in <sup>87</sup>Sr/<sup>86</sup>Sr could be controlled by the flow-route and level of interaction of the infiltrating water with silt and clay layers, which are more radiogenic compared to the carbonate host rock (Banner et al., 1996; Wortham et al., 2017). However, this would require a process that leads to changes in vadose flow routes, in turn depending on rainfall variations, and enhances the interaction with silt and clay layers. A diffuse flow through low porosity/permeability silicate layers during drier conditions would increase the Sr radiogenic signal, whereas a fracture flow through carbonate layers during wetter conditions would decrease this signal (Musgrove and Banner, 2004; Wortham et al., 2017). São Mateus cave is indeed situated in a geological setting where the limestone bedrock clearly intersects siliciclastic rocks (section 2, Supp. Fig. 2). This could explain the increased <sup>87</sup>Sr/<sup>86</sup>Sr ratios in SMT16 during the Early Holocene and the subsequent gradual decrease in <sup>87</sup>Sr/<sup>86</sup>Sr over the Holocene due to diminished interaction with these layers in the epikarst because of increasing local precipitation and different flow-routes. However, with the current data, this process is difficult to prove.

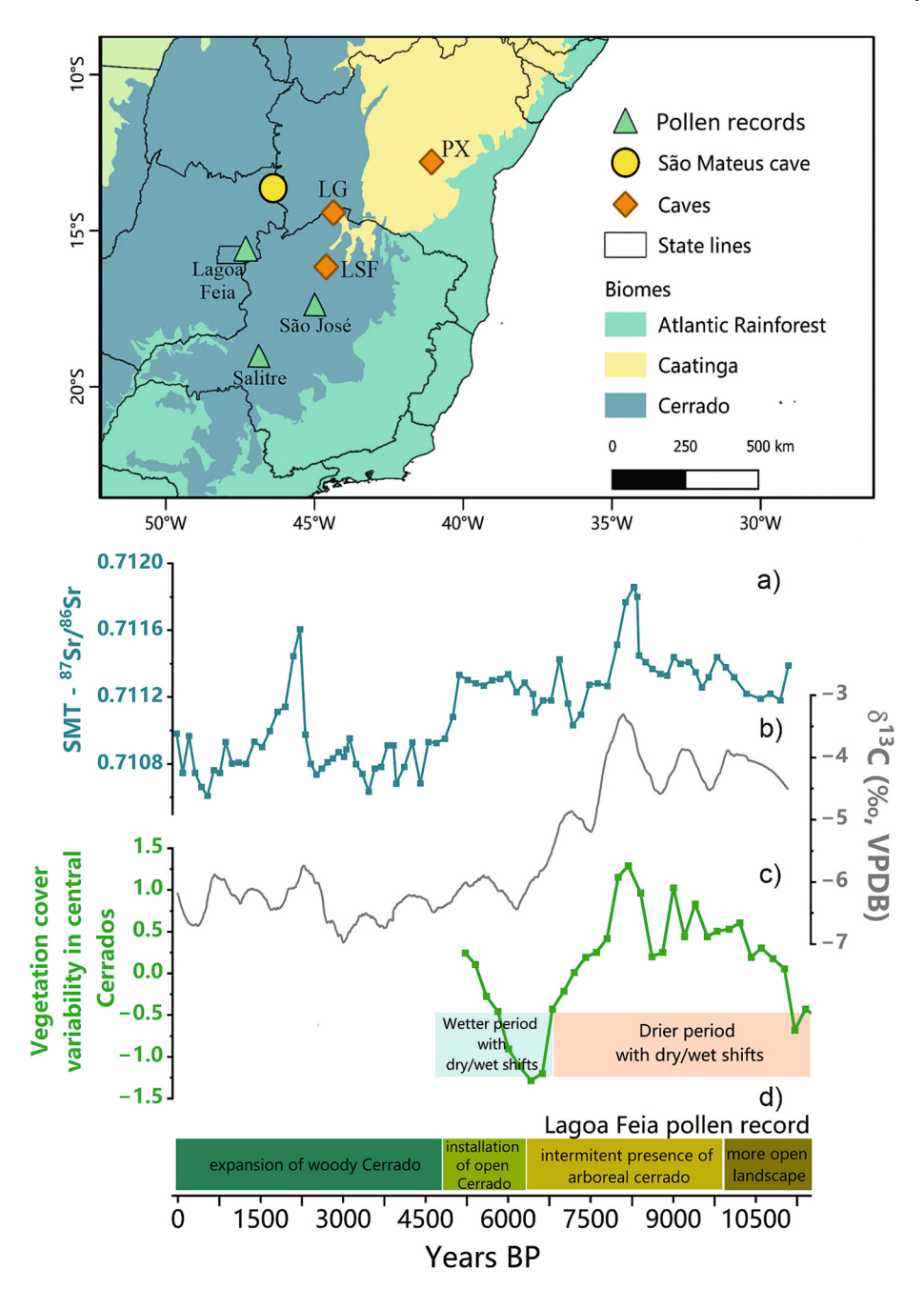


Fig. 4. (top) Map of central-eastern and northeastern Brazil records with the study sites discussed in the text: Paixão cave (Stríkis et al., 2015); Lapa Sem Fim cave (Azevedo et al., 2021); Lapa Grande cave (Stríkis et al., 2011); Lagoa Feia (Cassino et al., 2020); São José (Cassino et al., 2018); Salitre (Ledru et al., 1996). (bottom) Comparison between: a) SMT16 <sup>87</sup>Sr/<sup>86</sup>Sr record (blue squares); b) smoothed SMT16 δ<sup>13</sup>C record (gray); c) scores for vegetation cover variability curve performed by Cassino et al. (2020) representing vegetation trends in central Cerrado (green) with the correspondent climate interpretation; d) interpretation of Lagoa Feia pollen record from Cassino et al. (2020) and Escobar-Torrez et al. (2024). (For interpretation of the references to colour in this figure legend, the reader is referred to the web version of this article.)

Another mechanism to increase Sr isotope values of speleothems in dry conditions is the deposition of windblown dust, as already explored in other studies (Banner et al., 1996; Goede et al., 1998; Frumkin and Stein, 2004). Eolian dust deposition on the soils above the cave can readily change speleothem  $^{87}\text{Sr}/^{86}\text{Sr}$  ratios, as it provides weatherable material with potentially distinct  $^{87}\text{Sr}/^{86}\text{Sr}$  ratios (Banner et al., 1996; Frumkin and Stein, 2004; Torfstein et al., 2018; Cruz et al., 2021). The Urucuia Group sandstone unit, to the east of São Mateus cave, is a potential dust source with highly radiogenic Sr isotope ratios (0.7299  $\pm$  0.0001; Roland, 2018). Even today, in a semi humid climate around São Mateus cave, dust storms are reported by locals, especially in the dry

season. Therefore, in an overall drier regional setting at São Mateus cave during the Early Holocene with longer, more severe dry spells, much more frequent episodes of dust transportation may have occurred at our site. The generally drier environment and longer extent of the dry seasons might have enabled more intense weathering and greater dust mobilization from Urucuia's friable rocks towards the west (Supp. Fig. 1). The more radiogenic  $^{87}\mathrm{Sr}/^{86}\mathrm{Sr}$  from Urucuia sediments would then be an important allochthonous Sr source to the cave site and overprint the Sr signal of the water residence time in the epikarst when the highest  $\delta^{13}\mathrm{C}$  values in SMT16 indicate dry conditions (Fig. 3). During the Middle and Late Holocene, with the increase of precipitation

throughout the year, shorter dry seasons and more vegetation cover, the deposition of dust would be strongly reduced and contribute much less, if at all, to the  $^{87}\mathrm{Sr}/^{86}\mathrm{Sr}$  speleothem signal (Frumkin and Stein, 2004). Therefore, given the proximity to Urucuia group rock exposures, this mechanism might have been an important factor in the observed major changes in Sr isotope ratios between the Early and the Late Holocene.

Finally, the similar pattern of the SMT16  $\delta^{13}$ C values and  $^{87}$ Sr/ $^{86}$ Sr ratios with the vegetation variability curve from Cassino et al. (2020) (Fig. 4) shows how these three proxies could have co-varied at that time: the dry/wet episodes cause concomitant lower/higher local moisture, sparser/denser vegetation and higher/lower contribution of the more radiogenic Sr source, either by the different flow routes or the increased dust deposition. Cassino et al. (2020) suggest that a sequence of centennial-scale moisture oscillations occurred during this period leading to a repeated increase and decrease in arboreal Cerrado and dry forest cover along with changes in lake levels. Stríkis et al. (2011) also points out that central-eastern Brazil was affected by the rapid meltdown of ice caps in the Northern Hemisphere that led to abrupt wet events in tropical South America until about 7000 BP. Since soil moisture is the main factor driving arboreal cover in Cerrado regions (de Assis et al., 2011; de Terra et al., 2018), this is consistent with the oscillations observed in SMT16  $\delta^{13}$ C and the  $^{87}$ Sr/ $^{86}$ Sr ratios.

# 5.3. Long-term evolution of Central-Eastern Brazil speleothem $\delta^{18}{\rm O}$ values during the Holocene

Considering the long-term drier-to-wetter trend in local hydroclimate conditions during the Holocene in central-east Brazil, the remaining question is what drives the long-term increase in SMT16  $\delta^{18}$ O values. The  $\delta^{18}$ O values of speleothems from the São Mateus cave region have been interpreted as a proxy for rainfall amount related to SACZ activity in central Brazil, where lower  $\delta^{18}\text{O}$  values are associated to a stronger SACZ and consequently wetter conditions, and vice versa for higher  $\delta^{18}$ O values (Moquet et al., 2016; Novello et al., 2018, also see section 5.1.3). Therefore, the long-term increase in the SMT16  $\delta^{18}$ O values throughout the Holocene would indicate a progressively lower contribution of the SACZ and consequently drier conditions. The processes controlling the  $\delta^{13}C$  and  $\delta^{18}O$  values in tropical regions affect both proxies in the same direction, typically resulting in a positive correlation (Novello et al., 2021). Yet, the long-term increase in the SMT16  $\delta^{18}$ O values throughout the Holocene is opposite to the scenario described above based on the  $\delta^{13}$ C values.

The spearman running correlation between the SMT16  $\delta^{13} C$  and  $\delta^{18} O$  records on shorter time-scale intervals reveals a non-stationary correlation through time with a negative correlation during the Early Holocene (r average of -0.2) and a positive one after  $\sim\!6500$  years BP, mostly ranging between 0.2 and 0.4 (Supp. Fig. 5). This demonstrates that while a negative correlation characterizes the long record (r = -0.5), a positive correlation between oxygen and carbon isotopes is present on the millennial time-scale during the mid-Middle Holocene to Late Holocene, agreeing with the correlations observed for tropical South America speleothem  $\delta^{13} C$  and  $\delta^{18} O$  records (Novello et al., 2021). This analysis also shows that the correlation between  $\delta^{13} C$  and  $\delta^{18} O$  is non-stationary throughout the Holocene. However, since the focus of this paper is on the long-term trends over the Holocene, millennial-scale variations are not discussed in detail here.

During this period, several studies from central Brazil observed a detachment between SACZ activity and local rainfall conditions (Wortham et al., 2017; Ward et al., 2019; Novello et al., 2019; Gorenstein et al., 2022). This suggests that the long-term trends in the  $\delta^{18}$ O records from the region reflect the supra-regional effect of the SACZ, i.e., its changing intensity and spatial variability (Novello et al., 2018; Wong et al., 2021; Gorenstein et al., 2022), and/or a source effect (Wortham et al., 2017; Bao et al., 2023) rather than solely amount effect, even if this is the case now for interannual and decadal averages documented for present day conditions (Moquet et al., 2016).

Existing  $\delta^{18}O$  records from central-east Brazil do not appear to be strongly influenced by the increase in insolation (Fig. 5a) (Wong et al., 2021). The ANG record, near to our study site, that covers the last 6800 years, and the LSF and LG records located more southwards (Fig. 1) do not present major trends in their  $\delta^{18}O$  records (Fig. 5a), which was interpreted as a relatively constant SACZ activity throughout the Holocene. In fact, the SMT16  $\delta^{18}O$  values also do not show an insolation trend during this period after 6800 years BP. However, the SMT16  $\delta^{18}O$  record is longer than the adjacent  $\delta^{18}O$  record of ANG, revealing that the trend towards higher  $\delta^{18}O$  values begins in the Early Holocene and lasts until the end of the Middle Holocene (Fig. 5a). Therefore, Wong et al. (2021) did not find a good relationship with the insolation trend because their record is much shorter than SMT16. Nonetheless, this increase in  $\delta^{18}O$  values is not visible in the central-eastern records slightly south that also expand into the Early Holocene (LG and LSF, Fig. 3).

The evolution of the SASM/SACZ systems during the Holocene on a transect of speleothem records between northeast and southeast Brazil (Fig. 5a) shows a consistent opposite pattern in the trends of the  $\delta^{18}$ O values between the Rio Grande do Norte record in NE Brazil (RN - Cruz et al., 2009) and the Botuverá record in SE Brazil (BTV - Wang et al., 2007; Bernal et al., 2016). The increase in austral summer insolation from Early-to-Late Holocene leads to the intensification of the SASM in western Amazonia (van Breukelen et al., 2008; Bird et al., 2011) that reaches south and southeast Brazil (BTV) and leads to a drying in northeastern Brazil (RN site) (Fig. 1), clearly evidencing the dipole pattern during the Holocene (Bernal et al., 2016; Utida et al., 2020; Cruz et al., 2009) (Fig. 5a). The trend in the SMT16  $\delta^{18}$ O record is broadly concomitant with insolation and appears to resemble, even if to a lesser degree, the δ<sup>18</sup>O trend of the records in NE Brazil, such as RN and particularly Paixão cave (PX - Stríkis et al., 2015), located ~600 km to the east of São Mateus cave (Figs. 4 and 5a). This suggests that, even though the São Mateus cave area is at the northern margin of the SACZ, it is located between the dipole boundaries and can still be influenced by the climate patterns from northeast Brazil, capturing a unique signal that is not seen in the other central-eastern records.

This shows that the SMT16  $\delta^{18}O$  record in fact reflects the supraregional effect of the SACZ and its spatial variation, but does not clarify the underlying issue of the local hydroclimate conditions. Backtrajectory analysis performed for São Mateus cave site shows the two distinct moisture sources that feed the SACZ. One from a more northeastward position following the pattern of monsoon onshore flow originating in the equatorial Atlantic Ocean (EAO), and a second one coming via westerly trade winds from the South Atlantic Ocean (SAO) (Fig. 5b). This demonstrates that, even for present-day conditions, there are two moisture trajectories bringing moisture to the area, suggesting that the  $\delta^{18}O_{\text{precip}}$  signatures can also be affected by other factors in the region, such as a source effect (Bao et al., 2023). Yet, it is observed that the local amount effect currently plays an important role (Moquet et al., 2016) and there is a dominant trajectory in place (Fig. 5b, Supp. Fig. 6). Although this effect is not investigated in the monitoring study performed by Moquet et al. (2016), it could be considered as an important mechanism, particularly for longer time scales (e.g., multi-millennial), where a different configuration of atmospheric circulation might have been in place, such as during the Early-and-Middle Holocene period (e.g. Wolf et al., 2023). The low insolation and resultant weaker SASM may have altered the atmospheric circulation patterns as we understand them today (Gorenstein et al., 2022), affecting the direction and intensity of moisture trajectories compared to the ones currently observed.

The low SMT16  $\delta^{18}$ O values during the Early Holocene could reflect then a higher influence of the EAO moisture source over the area. As revealed by previous studies (Cruz et al., 2009; Utida et al., 2020), the humidity in the NE region has an anti-phase relationship with the SASM/SACZ regions during the Holocene, presenting wetter conditions during the Early-Middle Holocene given that the ITCZ (EAO source) was more active over NE Brazil during this period, whereas SASM records present drier conditions. Since the coupling between local humidity and

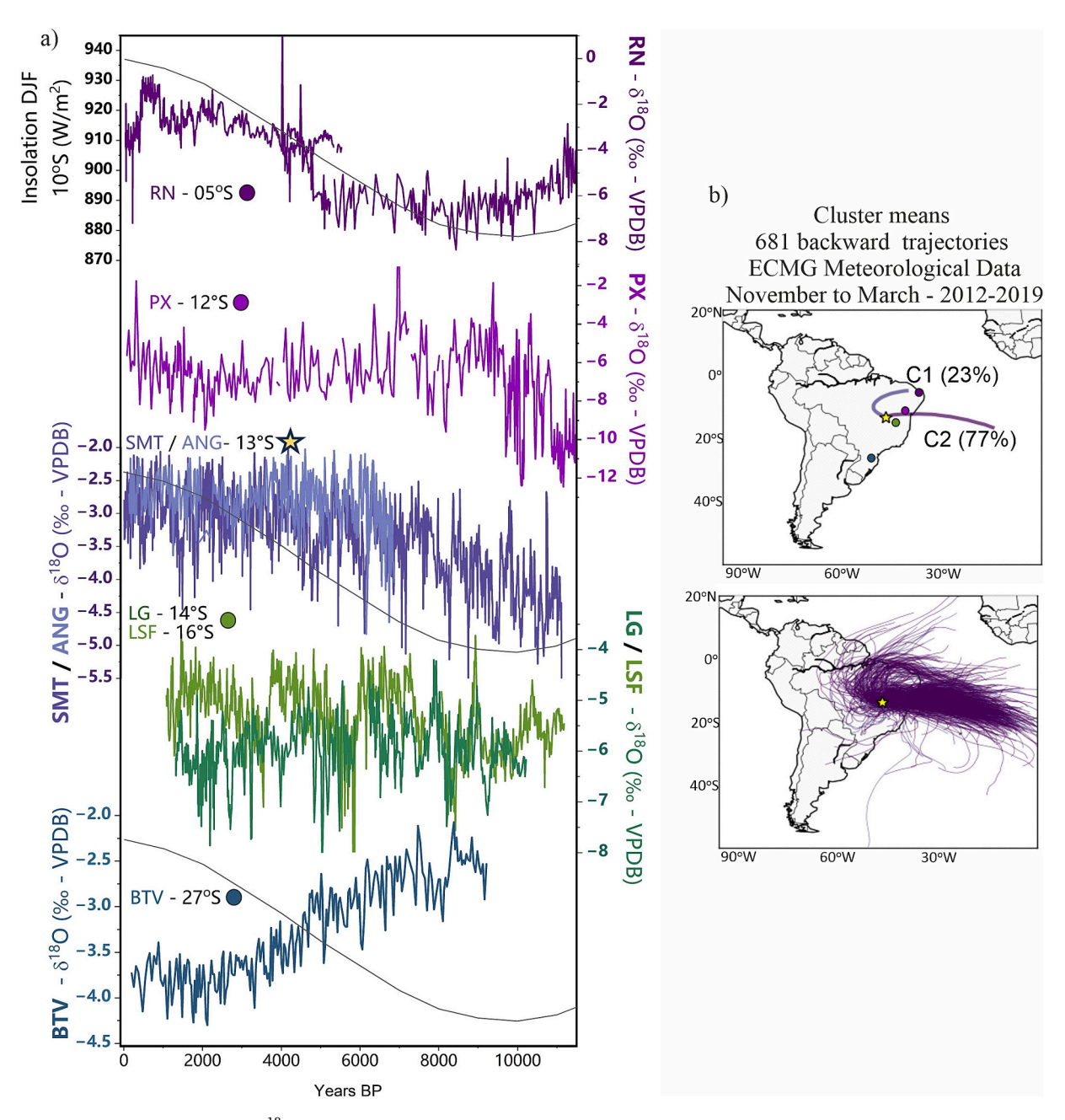


Fig. 5. a) NE-SE South America transect of  $\delta^{18}$ O records. Top to bottom: Rio Grande do Norte (Cruz et al., 2009); Paixão cave (Stríkis et al., 2015); São Mateus cave (this study); Lapa Sem Fim cave (Azevedo et al., 2021); Lapa Grande (Stríkis et al., 2011); Botuverá cave (Wang et al., 2007). Insolation curve for  $10^{\circ}$ S shown in black, with increasing values to the top. b) Clusters of 7-day back-trajectories (top) Mean back-trajectories for each cluster with their frequency (C1, C2); regarding the origin, the trajectories can be sorted in North-East (C1) and East (C2). Dots represent each cave site mentioned above. (bottom) All back-trajectories corresponding to top panel.

atmospheric variability is well-established at RN (Utida et al., 2020; Cruz et al., 2009), the RN  $\delta^{18}O$  and  $\delta^{13}C$  records suggest increased precipitation in the northeast region during the Early Holocene and the Middle Holocene given the concomitant low  $\delta^{18}O$  and  $\delta^{13}C$  values (Figs. 5 and 3, respectively) with the presence of Cerrado vegetation and a longer rain season (Utida et al., 2020). Therefore, a more southern position of the ITCZ during the Early and the mid-Middle Holocene must have strengthened the EAO moisture source, which already has a more depleted  $\delta^{18}O_{precip}$  signal (Supp. Fig. 7), and since São Mateus cave is located further south, it may have been further depleted when it reached the cave site due to the degree of rainout upstream (Bao et al., 2023). As insolation gradually increased after the Middle Holocene, these patterns likely reorganized, leading to the progressive shift to the major

contribution of the more enriched SAO moisture source (Supp. Fig. 7) and the establishment of the current SACZ system after  $\sim$ 6500 BP.

Moreover, as observed in the PX  $\delta^{18}$ O and  $\delta^{13}$ C records, the Early Holocene also shows extremely low values (Fig. 5a), and the pollen record from Icatu River (De Oliveira et al., 1999 – Fig. 1) is the only one around SMT that evidences gallery and tropical humid forest and a wet period during Early Holocene until ~6700 BP. Thus, the low SMT16  $\delta^{18}$ O values do not necessarily reflect the actual rainfall amount at the cave site for the Early and mid-Middle Holocene, but instead the intermittent influence of the EAO source. This demonstrates how, on the one hand, the SMT16  $\delta^{13}$ C record follows the overall drier-to-wetter hydroclimate trend observed in other SASM sites throughout the Holocene, along with the other central records LSF and LG (Figs. 3 and 4),

where the SASM activity gets stronger with increasing insolation (Bernal et al., 2016). On the other, the SMT16  $\delta^{18}$ O record seems to be also influenced by atmospheric changes that lead to similar  $\delta^{18}$ O pattern to the NE region and to a certain degree reflects this opposite pattern during the Early Holocene (Fig. 5a).

#### 6. Conclusions

The SMT16  $\delta^{13}$ C record reveals a drier than present scenario during the early and mid-Holocene, in agreement with other regional speleothem  $\delta^{13}$ C records and pollen data from central Brazil. This suggests an increase of water availability in the region throughout the Holocene associated with a denser vegetation. The strong positive correlation between the SMT16  $\delta^{13}$ C values and  $^{87}$ Sr/ $^{86}$ Sr ratios indicates that a similar geochemical process or environmental setting affected these proxies during the Holocene, which is, however, different from the classical interpretations. Still, the <sup>87</sup>Sr/<sup>86</sup>Sr ratios imply changes in local hydrology, where more (less) radiogenic values occur during drier (wetter) periods. We propose two mechanisms that may account for this: 1) how infiltrating water interacts with more radiogenic silt and clayey layers in the bedrock during drier periods compared to wetter periods, with diffuse flow through less permeable silicate layers increasing the radiogenic signal, while fracture flow through carbonate layers during wet conditions resulting in a decrease in the Sr ratio; 2) increased input of windblown dust from a more radiogenic source (Urucuia sandstone unit) during drier periods with sparser vegetation would increase the speleothem Sr isotope ratios, while reduced input from this source during wetter periods and denser vegetation would result in less radiogenic signatures closer to the limestone bedrock. This highlights that Sr isotopes are a site-specific proxy and local settings should be

The long-term trend of the SMT  $\delta^{18}$ O record is consistent with large scale δ<sup>18</sup>O patterns in South America. However, this long-term trend responds to both variations in local moisture and the degree of rainout upstream that occurs during the moisture transport from the ocean to the cave site. From the Early-to-Late Holocene, it follows the increase in austral summer insolation, similar to records from NE Brazil, reaching a plateau during the Late Holocene similar to other SACZ records. The low insolation and a resulting weak monsoon system during the early and Middle Holocene enabled rapid climate variability and different atmospheric conditions than observed today. Therefore, the SMT area was possibly more strongly influenced by other moisture sources from the NE, and the lower  $\delta^{18}$ O values resulted from the degree of rainout upstream of the air masses reaching the area during this time. With the progressive increase in insolation and the re-establishment of the monsoon system, the influence from the South Atlantic source increased, as observed in the modern-day back trajectory analysis, which contributes to the formation of the SACZ.

# CRediT authorship contribution statement

Marcela Eduarda Della Libera: Writing – review & editing, Writing – original draft, Visualization, Investigation, Data curation, Conceptualization. Julio Cauhy: Writing – review & editing, Writing – original draft, Investigation, Conceptualization. Cintia Stumpf: Writing – review & editing, Validation, Formal analysis, Data curation, Conceptualization. Roberto V. Santos: Resources, Funding acquisition. Francisco W. Cruz: Writing – review & editing, Resources, Formal analysis. Nicolas M. Stríkis: Writing – review & editing. Luciana F. Prado: Validation, Resources. Jean-Sebastian Moquet: Methodology, Formal analysis, Data curation, Conceptualization. Michael Weber: Writing – review & editing, Formal analysis, Data curation. Rebecca Orrison: Writing – review & editing, Data curation. Hai Cheng: Resources. R. Lawrence Edwards: Resources. Valdir F. Novello: Writing – review & editing, Supervision, Investigation. Hubert Vonhof: Writing – review & editing, Supervision, Resources, Conceptualization. Denis

**Scholz:** Writing – review & editing, Supervision, Funding acquisition, Formal analysis, Conceptualization.

# **Declaration of competing interest**

The authors declare that they have no known competing financial interests or personal relationships that could have appeared to influence the work reported in this paper.

# Acknowledgements

We acknowledge financial support for this project from the Max Planck Graduate Center Mainz, the Deutsche Forschungsgemeinschaft through grant INST 247/889-1 FUGG to DS. We also acknowledge the support from Coordenação de Aperfeiçoamento de Pessoal de Nível Superior (CAPES) through the master's scholarship (process number 1715493) to C.F. Stumpf., Conselho Nacional de Desenvolvimento Científico e Tecnológico (CNPq) to R.V. Santos (grant 310641/2014-4) and FAPESP grants 2017/50085-3 to F.W-C and 2011/12238-6 to J.S.M. We would also like to thank Sr. Ramiro for the assistance in the field work.

#### Appendix A. Supplementary data

Supplementary data to this article can be found online at https://doi.org/10.1016/j.gloplacha.2025.105186.

#### Data availability

The new  $\delta^{18}O,\,\delta^{13}C$  and  $^{87}Sr/^{86}Sr$  records from São Mateus cave will be available at PANGAEA.

# References

- Ampuero, A., Stríkis, N.M., Apaéstegui, J., Vuille, M., Novello, V.F., Espinoza, J.C., Cruz, F.W., Vonhof, H., Mayta, V.C., Martins, V.T.S., Cordeiro, R.C., Azevedo, V., Sifeddine, A., 2020. The Forest Effects on the Isotopic Composition of Rainfall in the Northwestern Amazon Basin. J. Geophys. Res.-Atmos. 125, e2019JD031445. https://doi.org/10.1029/2019JD031445.
- Auler, A., Farrant, A.R., 1996. A brief introduction to karst and caves in Brazil. Proc. Univ. Bristol Splaeol. Soc. 20, 187–200. In: https://www.ubss.org.uk/resources/proceedings/vol20/UBSS\_Proc\_20\_3\_187-200.pdf (accesses 22 September 2025).
- Azevedo, V., Strikis, N.M., Novello, V.F., Roland, C.L., Cruz, F.W., Santos, R.V., Vuille, M., Utida, G., De Andrade, F.R.D., Cheng, H., Edwards, R.L., 2021. Paleovegetation seesaw in Brazil since the late Pleistocene: a multiproxy study of two biomes. Earth Planet. Sci. Lett. 563, 116880. https://doi.org/10.1016/j.epsl.2021.116880.
- Banner, J.L., Musgrove, M., Asmerom, Y., Lawrence Edwards, R., Hoff, J.A., 1996. High-resolution temporal record of Holocene ground-water chemistry: Tracing links between climate and hydrology. Geology 24, 1049–1053. https://doi.org/10.1130/0091-7613(1996)024<1049:HRTROH>2.3.CO;2.
- Bao, Y., Liu, Z., He, C., 2023. Dipole response of Millennial variability in Tropical South American precipitation and δ<sup>18</sup>O<sub>p</sub> during the Last Deglaciation. Part II: δ<sup>18</sup>O<sub>p</sub> response. J. Clim. 36, 4709–4721. https://doi.org/10.1175/JCLI-D-22-0289.1.
- Barberi, M., Salgado-Labouriau, M.L., Suguio, K., 2000. Paleovegetation and paleoclimate of "Vereda de Águas Emendadas", Central Brazil. J. S. Am. Earth Sci. 13 (3), 241–254. https://doi.org/10.1016/S0895-9811(00)00022-5.
- Behling, H., 2002. Late Quaternary vegetation and climate dynamics in southeastern Amazonia inferred from Lagoa da Confusão in Tocantins State, northern Brazil. Amazoniana XVII 27–40.
- Berger, A., Loutre, M.F., 1991. Insolation values for the climate of the last 10 million years. Quat. Sci. Rev. 10 (4), 297–317. https://doi.org/10.1016/0277-3791(91)
- Bernal, J.P., Cruz, F.W., Stríkis, N.M., Wang, X., Deininger, M., Catunda, M.C.A., Ortega-Obregón, C., Cheng, H., Edwards, R.L., Auler, A.S., 2016. High-resolution Holocene South American monsoon history recorded by a speleothem from Botuverá Cave, Brazil. Earth Planet. Sci. Lett. 450, 186–196. https://doi.org/10.1016/j.epsl.2016.06.008.
- Bird, B.W., Abbott, M.B., Rodbell, D.T., Vuille, M., 2011. Holocene tropical South American hydroclimate revealed from a decadally resolved lake sediment δ<sup>18</sup>O record. Earth Planet. Sci. Lett. 310, 192–202. https://doi.org/10.1016/j. epsl.2011.08.040.
- Bustamante, M., Nardoto, G.B., Pinto, A.S., Resende, J.C.F., Takahashi, F.S.C., Vieira, L. C.G., 2012. Potential impacts of climate change on biogeochemical functioning of Cerrado ecosystems. Braz. J. Biol. 72 (3), 655–671. https://doi.org/10.1590/S1519-69842012000400005.

- Campos, J., Dardenne, M.A., 1997. Estratigrafia e Sedimentação da Bacia Sanfranciscana: Uma Revisão. Ver. Brasil. Geocienc. 27, 269–282. https://ppegeo.igc.usp.br/portal/index.php/rbg/estratigrafia-e-sedimentacao-da-bacia-sanfranciscana-uma-revisao/(accessed 22 September 2025).
- Campos, J.L.P.S., Cruz, F.W., Ambrizzi, T., Deininger, M., Vuille, M., Novello, V.F., Strikis, N.M., 2019. Coherent South American Monsoon variability during the last millennium revealed through high-resolution proxy records. Geophys. Res. Lett. 46, 8261–8270. https://doi.org/10.1029/2019GL082513.
- Cassino, R.F., Martinho, C.T., da Silva Caminha, S.A.F., 2018. A late Quaternary palynological record of a palm swamp in the Cerrado of Central Brazil interpreted using modern analog data. Palaeogeogr. Palaeoclimatol. Palaeoecol. 490, 1–16. https://doi.org/10.1016/j.palaeo.2017.08.036.
- Cassino, R.F., Ledru, M.P., de Santos, R.A., Favier, C., 2020. Vegetation and fire variability in the central Cerrados (Brazil) during the Pleistocene-Holocene transition was influenced by oscillations in the SASM boundary belt. Quat. Sci. Rev. 232, 106209. https://doi.org/10.1016/j.quascirev.2020.106209.
- Cheng, H., Sinha, A., Cruz, F.W., Wang, X., Edwards, R.L., D'Horta, F.M., Ribas, C.C., Vuille, M., Stott, L.D., Auler, A.S., 2013. Climate change patterns in Amazonia and biodiversity. Nat. Commun. 4, 1411. https://doi.org/10.1038/ncomms2415.
- Cruz, F.W., Vuille, M., Burns, S.J., Wang, X., Cheng, H., Werner, M., Edwards, R.L., Karmann, I., Auler, A.S., Nguyen, H., 2009. Orbitally driven east-west antiphasing of South American precipitation. Nat. Geosci. 2, 210–214. https://doi.org/10.1038/ pge0444
- Cruz, J.A., Mcdermott, F., Turrero, M.J., Edwards, R.L., Martín-Chivelet, J., 2021. Strong links between Saharan dust fluxes, monsoon strength, and North Atlantic climate during the last 5000 years. Sci. Adv. 27, eabe6102. https://doi.org/10.1126/sciadv. abe6102.
- Dardenne, M.A., 1978. Síntese sobre a estratigrafia do Grupo Bambuí no Brasil Central. In: Anais do XXX Congr. Bras. de Geol. Recife, pp. 597–610.
- de Assis, A.C.C., Coelho, R.M., da Pinheiro, E.S., Durigan, G., 2011. Water availability determines physiognomic gradient in an area of low-fertility soils under Cerrado vegetation. Plant Ecol. 212, 1135–1147. https://doi.org/10.1007/s11258-010-9893-8.
- De Oliveira, P.E., Magnólia, A., Barreto, F., Suguio, K., 1999. Late Pleistocene/Holocene climatic and vegetational history of the Brazilian caatinga: the fossil dunes of the middle S\u00e4o Francisco River. Palaeogeogr. Palaeoclimatol. Palaeoecol. 152, 319–337. https://doi.org/10.1016/S0031-0182(99)00061-9.
- de Terra, M.C.N.S., Dos Santos, R.M., Júnior, Prado, Do, J.A., De Mello, J.M., Scolforo, J. R.S., Fontes, M.A.L., Schiavini, I., Dos Reis, A.A., Bueno, I.T., Magnago, L.F.S., Ter Steege, H., 2018. Water availability drives gradients of tree diversity, structure and functional traits in the Atlantic-Cerrado-Caatinga transition, Brazil. J. Plant Ecol. 11, 803–814. https://doi.org/10.1093/jpe/rty017.
- Deininger, M., Ward, B.M., Novello, V.F., Cruz, F.W., 2019. Late quaternary variations in the south american monsoon system as inferred by speleothems—new perspectives using the SISAL database. Quaternary 2 (1), 6. https://doi.org/10.3390/ quat2010006.
- Della Libera, M.E., Novello, V.F., Cruz, F.W., Orrison, R., Vuille, M., Maezumi, S.Y., de Souza, J., Cauhy, J., Campos, J.L.P.S., Ampuero, A., Utida, G., Stríkis, N.M., Stumpf, C.F., Azevedo, V., Zhang, H., Edwards, R.L., Cheng, H., 2022. Paleoclimatic and paleoenvironmental changes in Amazonian lowlands over the last three millennia. Quat. Sci. Rev. 279, 107383. https://doi.org/10.1016/J. OUASCIREV.2022.107383.
- Edwards, R.L., Chen, J., Wasserburg, G., 1987. <sup>238</sup>U-<sup>234</sup>U-<sup>230</sup>Th-<sup>232</sup>Th systematics and the precise measurement of time over the past 500,000 years. Earth Planet. Sci. Lett. 81, 175–192. https://doi.org/10.1016/0012-821X(87)90154-3.
- Escobar-Torrez, K., Ledru, M.P., Cassino, R.F., Bianchini, P.R., Yokoyama, E., 2024. Long-and short-term vegetation change and inferred climate dynamics and anthropogenic activity in the central Cerrado during the Holocene. J. Quat. Sci. 39, 130–144. https://doi.org/10.1002/jqs.3567.
- Fairchild, I.J., Baker, A., 2012. Speleothem Science: From Process to Past Environments, First ed. Wiley-Blackwell, West Sussex.
- Fohlmeister, J., Scholz, D., Kromer, B., Mangini, A., 2011. Modelling carbon isotopes of carbonates in cave drip water. Geochim. Cosmochim. Acta 75, 5219–5228. https:// doi.org/10.1016/j.gca.2011.06.023.
- Fohlmeister, J., Riavo, G., Voarintsoa, N., Lechleitner, F.A., Boyd, M., Brandtstätter, S., Jacobson, M.J., Oster, J., 2020. Main controls on the stable carbon isotope composition of speleothems. Geochim. Cosmochim. Acta 279, 67–87. https://doi.org/10.1016/j.gca.2020.03.042.
- Frumkin, A., Stein, M., 2004. The Sahara-East Mediterranean dust and climate connection revealed by strontium and uranium isotopes in a Jerusalem speleothem. Earth Planet. Sci. Lett. 217, 451–464. https://doi.org/10.1016/S0012-821X(03) 00589-2
- Funk, C.C., Peterson, P.J., Landsfeld, M.F., Pedreros, D.H., Verdin, J.P., Rowland, J.D., Romero, B.E., Husak, G.J., Michaelsen, J.C., Verdin, A.P., 2014. A quasi-global precipitation time series for drought monitoring. U.S. Geolog. Surv. Data Ser. 832, 1–4. https://doi.org/10.3133/ds832.
- Garreaud, R.D., Vuille, M., Compagnucci, R., Marengo, J., 2009. Present-day South American climate. Palaeogeogr. Palaeoclimatol. Palaeoecol. 281, 180–195. https://doi.org/10.1016/j.palaeo.2007.10.032.
- Goede, A., Mcculloch, M., Mcdermott, F., Hawkesworth, C., 1998. Aeolian contribution to strontium and strontium isotope variations in a Tasmanian speleothem. Chem. Geol. 149, 37–50. https://doi.org/10.1016/S0009-2541(98)00035-7.
- Gorenstein, I., Prado, L.F., Bianchini, P.R., Wainer, I., Griffiths, M.L., Pausata, F.S.R., Yokoyama, E., 2022. A fully calibrated and updated mid-Holocene climate reconstruction for Eastern South America. Quat. Sci. Rev. 292, 107646. https://doi. org/10.1016/j.quascirev.2022.107646.

- Gouveia, S.E.M., Pessenda, L.C.R., Aravena, R., Boulet, R., Scheel-Ybert, R., Bendassoli, J. A., Ribeiro, A.S., Freitas, H.A., 2002. Carbon isotopes in charcoal and soils in studies of paleovegetation and climate changes during the late Pleistocene and the Holocene in the southeast and centerwest regions of Brazil. Glob. Planet. Chang. 33, 95–106. https://doi.org/10.1016/S0921-8181(02)00064-4.
- Governo do Estado de Goiás, Secretaria de Meio Ambiente e Desenvolvimento Sustentável, STCP Engenharia de Projetos Ltda, 2016. Guia rápido de aplicação: Plano de Manejo Espeleológico Parque Estadual de Terra Ronca. Retrieved from. https://goias.gov.br/meioambiente/wp-content/uploads/sites/33/2016/06/PME\_PETER\_Guia\_Final\_revisao-e98.pdf (accessed 22 September 2025).
- Hersbach, H., Bell, B., Berrisford, P., Hirahara, S., Horányi, A., Muñoz-Sabater, J., Nicolas, J., Peubey, C., Radu, R., Schepers, D., Simmons, A., Soci, C., Abdalla, S., Abellan, X., Balsamo, G., Bechtold, P., Biavati, G., Bidlot, J., Bonavita, M., De Chiara, G., Dahlgren, P., Dee, D., Diamantakis, M., Dragani, R., Flemming, J., Forbes, R., Fuentes, M., Geer, A., Haimberger, L., Healy, S., Hogan, R.J., Hólm, E., Janisková, M., Keeley, S., Laloyaux, P., Lopez, P., Lupu, C., Radnoti, G., de Rosnay, P., Rozum, I., Vamborg, F., Villaume, S., Thépaut, J.N., 2020. The ERA5 global reanalysis. Q. J. R. Meteorol. Soc. 146, 1999–2049. https://doi.org/10.1002/gi.3803
- Hofmann, G.S., Silva, R.C., Weber, E.J., Barbosa, A.A., Oliveira, L.F.B., Alves, R.J.V., Hasenack, H., Schossler, V., Aquino, F.E., Cardoso, M.F., 2023. Changes in atmospheric circulation and evapotranspiration are reducing rainfall in the Brazilian Cerrado. Sci. Rep. 13, 11236. https://doi.org/10.1038/s41598-023-38174-x.
- Huffman, G.J., Bolvin, D.T., Joyce, R., Nelkin, E.J., Tan, J., Braithwaite, D., Hsu, K.,
   Kelley, O.A., Nguyen, P., Sorooshian, S., Watters, D.C., West, B.J., Xie, P., 2023.
   Algorithm Theoretical Basis Document (ATBD) NASA Global Precipitation
   Measurement (GPM) Integrated Multi-satellite Retrievals for GPM (IMERG) (Version 07)
- Hurley, J.V., Galewsky, J., Worden, J., Noone, D., 2012. A test of the advection-condensation model for subtropical water vapor using stable isotopologue observations from Mauna Loa Observatory, Hawaii. J. Geophys. Res. Atmos. 117, D19118. https://doi.org/10.1029/2012JD018029.
- Klink, C.A., Sato, M.N., Cordeiro, G.G., Ramos, M.I.M., 2020. The role of vegetation on the dynamics of water and fire in the Cerrado ecosystems: Implications for management and conservation. Plants 9, 1803. https://doi.org/10.3390/ plants9121803.
- Ledru, M.-P., Braga, P.I.S., Soubiès, F., Fournier, M., Martin, L., Suguio, K., Turcq, B., 1996. The last 50,000 years in the Neotropics (Southern Brazil): evolution of vegetation and climate. Palaeogeogr. Palaeoclimatol. Palaeoecol. 123, 239–257. https://doi.org/10.1016/0031-0182(96)00105-8.
- Lenters, J.D., Cook, K.H., 1997. On the origin of the Bolivian high and related circulation features of the South American climate. J. Atmos. Sci. 54, 656–677. https://doi.org/ 10.1175/1520-0469(1997)054<0656:OTOOTB>2.0.CO;2.
- Marengo, J.A., Liebmann, B., Grimm, A.M., Misra, V., Silva Dias, P.L., Cavalcanti, I.F.A., Carvalho, L.M.V., Berbery, E.H., Ambrizzi, T., Vera, C.S., Saulo, A.C., Nogues-Paegle, J., Zipser, E., Seth, A., Alves, L.M., 2012. Recent developments on the South American monsoon system. Int. J. Climatol. 32, 1–21. https://doi.org/10.1002/ joc.2254.
- McDermott, F., 2004. Palaeo-climate reconstruction from stable isotope variations in speleothems: a review. Quat. Sci. Rev. 23, 901–918. https://doi.org/10.1016/j. quascirev.2003.06.021.
- Moquet, J.S., Cruz, F.W., Novello, V.F., Stríkis, N.M., Deininger, M., Karmann, I., Santos, R.V., Millo, C., Apaestegui, J., Guyot, J.L., Siffedine, A., Vuille, M., Cheng, H., Edwards, R.L., Santini, W., 2016. Calibration of speleothem δ<sup>18</sup>O records against hydroclimate instrumental records in Central Brazil. Glob. Planet. Chang. 139, 151–164. https://doi.org/10.1016/j.gloplacha.2016.02.001.
- Musgrove, M.L., Banner, J.L., 2004. Controls on the spatial and temporal variability of vadose dripwater geochemistry: Edwards aquifer, Central Texas. Geochim. Cosmochim. Acta 68, 1007–1020. https://doi.org/10.1016/j.gca.2003.08.014.
- Novello, V.F., Cruz, F.W., Moquet, J.S., Vuille, M., de Paula, M.S., Nunes, D., Edwards, R. L., Cheng, H., Karmann, I., Utida, G., Stríkis, N.M., Campos, J.L.P.S., 2018. Two Millennia of South Atlantic Convergence Zone variability reconstructed from Isotopic Proxies. Geophys. Res. Lett. 45, 5045–5051. https://doi.org/10.1029/2017.61.076838
- Novello, V.F., Cruz, F.W., McGlue, M.M., Wong, C.I., Ward, B.M., Vuille, M., Santos, R.A., Jaqueto, P., Pessenda, L.C.R., Atorre, T., Ribeiro, L.M.A.L., Karmann, I., Barreto, E.S., Cheng, H., Edwards, R.L., Paula, M.S., Scholz, D., 2019. Vegetation and environmental changes in tropical South America from the last glacial to the Holocene documented by multiple cave sediment proxies. Earth Planet. Sci. Lett. 524, 115717. https://doi.org/10.1016/j.epsl.2019.115717.
- Novello, V.F., William da Cruz, F., Vuille, M., Pereira Silveira Campos, J.L., Stríkis, N.M., Apaéstegui, J., Moquet, J.S., Azevedo, V., Ampuero, A., Utida, G., Wang, X., Paula-Santos, G.M., Jaqueto, P., Ruiz Pessenda, L.C., Breecker, D.O., Karmann, I., 2021. Investigating 8<sup>13</sup>C values in stalagmites from tropical South America for the last two millennia. Quat. Sci. Rev. 255, 106822. https://doi.org/10.1016/j.quascirev.2021.106822.
- Orrison, R., Vuille, M., Smerdon, J.E., Apaéstegui, J., Leandro, S., Campos, J.P., Cruz, F. W., Della Libera, M.E., 2022. South American Monsoon variability over the last millennium in paleoclimate records and isotope-enabled climate models. Clim. Past 18, 2045–2062. https://doi.org/10.5194/cp-2022-6.
- Pessenda, L.C.R., Gouveia, S.E.M., de Ribeiro, A.S., De Oliveira, P.E., Aravena, R., 2010. Late Pleistocene and Holocene vegetation changes in northeastern Brazil determined from carbon isotopes and charcoal records in soils. Palaeogeogr. Palaeoclimatol. Palaeoecol. 297, 597–608. https://doi.org/10.1016/j.palaeo.2010.09.008.

- Rodwell, M.J., Hoskins, B.J., 2001. Subtropical anticyclones and Summer Monsoons.

  J. Clim. 14, 3192–3211. https://doi.org/10.1175/1520-0442(2001)014<3192:
  SAASM>20.00:2
- Roland, C.L., 2018. Utilização de análises isotópicas multiproxy (<sup>87</sup>Sr/<sup>86</sup>Sr,  $\delta^{234}$ U,  $\delta^{13}$ C,  $\delta^{18}$ O) na reconstrução paleoclimática e paleoambiental do centro-leste do Brasil, norte de Minas Gerais. Universidade Federal Fluminense.
- Rolph, G., Stein, A., Stunder, B., 2017. Real-time Environmental applications and Display sYstem: READY. Environ. Model. Softw. 95, 210–228. https://doi.org/10.1016/j.envsoft 2017.06.025
- Sabino, S.M.L., Cassino, R.F., Gomes, M.O.S., Sant'anna, E.M.E., Rocha Augustin, C.H.R., De Oliveira, D.A., 2021. Late Holocene in Central Brazil: vegetation changes and humidity variability in a tropical wetland. J. Quat. Sci. 36, 1028–1039. https://doi. org/10.1002/ins.3351.
- Salgado-Labouriau, M.L., Casseti, V., Ferraz-Vicentini, K.R., Martin, L., Soubies, F., Suguio, K., Turcq, B., 1997. Late Quaternary vegetational and climatic changes in Cerrado and palm swamp from Central Brazil. Palaeogeogr. Palaeoclimatol. Palaeoecol. 128, 215–226. https://doi.org/10.1016/S0031-0182(96)00018-1.
- Scholz, D., Hoffmann, D.L., 2011. StalAge an algorithm designed for construction of speleothem age models. Quat. Geochronol. 6, 369–382. https://doi.org/10.1016/j. quageo.2011.02.002.
- Smith, R.J., Mayle, F.E., 2018. Impact of mid- to late Holocene precipitation changes on vegetation across lowland tropical South America: a paleo-data synthesis. Quat. Res. (United States) 89, 134–155. https://doi.org/10.1017/qua.2017.89.
- Stein, A.F., Draxler, R.R., Rolph, G.D., Stunder, B.J.B., Cohen, M.D., Ngan, F., 2015. Noaa's hysplit atmospheric transport and dispersion modeling system. Bull. Am. Meteorol. Soc. 96, 2059–2077. https://doi.org/10.1175/BAMS-D-14-00110.1.
- Stríkis, N.M., Cruz, F.W., Cheng, H., Karmann, I., Edwards, R.L., Vuille, M., Wang, X., de Paula, M.S., Novello, V.F., Auler, A.S., 2011. Abrupt variations in South American monsoon rainfall during the Holocene based on a speleothem record from Central-Eastern Brazil. Geology 39, 1075–1078. https://doi.org/10.1130/G32098.1.
- Stríkis, N.M., Chiessi, C.M., Cruz, F.W., Vuille, M., Cheng, H., De Souza Barreto, E.A., Mollenhauer, G., Kasten, S., Karmann, I., Edwards, R.L., Bernal, J.P., Sales, H.D.R., 2015. Timing and structure of Mega-SACZ events during Heinrich Stadial 1. Geophys. Res. Lett. 42, 5477–5484. https://doi.org/10.1002/2015GL064048.
- Sulca, J., Vuille, M., Silva, Y., Takahashi, K., 2016. Teleconnections between the Peruvian Central Andes and Northeast Brazil during extreme rainfall events in austral summer. J. Hydrometeorol. 17, 499–515. https://doi.org/10.1175/JHM-D-15-0034 1
- Torfstein, A., Goldstein, S.L., Stein, M., 2018. Enhanced Saharan dust input to the Levant during Heinrich stadials. Quat. Sci. Rev. 186, 142–155. https://doi.org/10.1016/j. quascirev.2018.01.018.
- Utida, G., Cruz, F.W., Santos, R.V., Sawakuchi, A.O., Wang, H., Pessenda, L.C.R., Novello, V.F., Vuille, M., Strauss, A.M., Borella, A.C., Stríkis, N.M., Guedes, C.C.F., Dias De Andrade, F.R., Zhang, H., Cheng, H., Edwards, R.L., 2020. Climate changes in Northeastern Brazil from deglacial to Meghalayan periods and related environmental impacts. Quat. Sci. Rev. 250, 106655. https://doi.org/10.1016/j. quascirev.2020.106655.

- van Breukelen, M.R., Vonhof, H.B., Hellstrom, J.C., Wester, W.C.G., Kroon, D., 2008. Fossil dripwater in stalagmites reveals Holocene temperature and rainfall variation in Amazonia. Earth Planet. Sci. Lett. 275, 54–60. https://doi.org/10.1016/j. epsl 2008 07 060
- Vuille, M., Burns, S.J., Taylor, B.L., Cruz, F.W., Bird, B.W., Abbott, M.B., Kanner, L.C., Cheng, H., Novello, V.F., 2012. A review of the South American monsoon history as recorded in stable isotopic proxies over the past two millennia. Clim. Past 8, 1309–1321. https://doi.org/10.5194/cp-8-1309-2012.
- Wang, X., Auler, A.S., Edwards, R.L., Cheng, H., Ito, E., Wang, Y., Kong, X., Solheid, M., 2007. Millennial-scale precipitation changes in southern Brazil over the past 90,000 years. Geophys. Res. Lett. 34, L23701. https://doi.org/10.1029/2007GL031149.
- Wang, X., Edwards, R.L., Auler, A.S., Cheng, H., Kong, X., Wang, Y., Cruz, F.W., Dorale, J. A., Chiang, H.W., 2017. Hydroclimate changes across the Amazon lowlands over the past 45,000 years. Nature 541, 204–207. https://doi.org/10.1038/nature20787.
- Ward, B.M., Wong, C.I., Novello, V.F., McGee, D., Santos, R.V., Silva, L.C.R., Cruz, F.W., Wang, X., Edwards, R.L., Cheng, H., 2019. Reconstruction of Holocene coupling between the South America Monsoon System and local moisture variability from speleothem 8<sup>18</sup>O and 8<sup>7</sup>Sr/8<sup>6</sup>Sr records. Quat. Sci. Rev. 210, 51–63. https://doi.org/10.1016/j.quascirev.2019.02.019.
- Weber, M., Ligli, F., Jochum, K.P., Cipriani, A., Scholz, D., 2018. Calcium carbonate and phosphate reference materials for monitoring Bulk and Microanalytical Determination of Sr Isotopes. Geostand. Geoanal. Res. 42, 77–89. https://doi.org/ 10.1111/gr.12191.
- Weber, M., Tacail, T., Lugli, F., Clauss, M., Weber, K., Leichliter, J., Winkler, D.E., Mertz-Kraus, R., Tütken, T., 2020. Strontium Uptake and Intra-Population <sup>87</sup>Sr/<sup>86</sup>Sr Variability of Bones and Teeth—Controlled Feeding experiments with Rodents (*Rattus norvegicus, Cavia porcellus*). Front. Ecol. Evol. 42, 77–89. https://doi.org/10.3389/fevo.2020.569940.
- Wolf, A., Ersek, V., Braun, T., et al., 2023. Deciphering local and regional hydroclimate resolves contradicting evidence on the Asian monsoon evolution. Nat. Commun. 14, 5697. https://doi.org/10.1038/s41467-023-41373-9.
- Wong, M.L., Wang, X., Latrubesse, E.M., He, S., Bayer, M., 2021. Variations in the South Atlantic convergence Zone over the mid-to-late Holocene inferred from speleothem 8<sup>18</sup>O in Central Brazil. Quat. Sci. Rev. 270, 107178. https://doi.org/10.1016/j. quascirev.2021.107178.
- Wong, M.L., Battisti, D.S., Liu, X., Ding, Q., Wang, X., 2023. A North–South Dipole response of the South Atlantic convergence zone during the mid-holocene. Geophys. Res. Lett. 50, e2023GL105130. https://doi.org/10.1029/2023GL105130.
- Wortham, B.E., Wong, C.I., Silva, L.C.R., McGee, D., Montañez, I.P., Troy Rasbury, E., Cooper, K.M., Sharp, W.D., Glessner, J.J.G., Santos, R.V., 2017. Assessing response of local moisture conditions in Central Brazil to variability in regional monsoon intensity using speleothem <sup>87</sup>Sr/<sup>86</sup>Sr values. Earth Planet. Sci. Lett. 463, 310–322. https://doi.org/10.1016/j.epsl.2017.01.034.
- Zilli, M.T., Carvalho, L.M.V., Lintner, B.R., 2019. The poleward shift of South Atlantic Convergence Zone in recent decades. Clim. Dyn. 52, 2545–2563. https://doi.org/ 10.1007/s00382-018-4277-1.